2016 年臺灣國際科學展覽會
優勝作品專輯

作品編號　**100007**

參展科別　工程學

作品名稱　**Experimental Study on Vibration Mitigation of Structure by Utilizing Paraboloidal Tank Tuned Liquid Damper (TLD)**

得獎獎項　大會獎：一等獎

就讀學校　國立臺南第一高級中學

指導教師　唐啟釗、黃進坤

作者姓名　陳彥辰

關鍵字　**Paraboloidal Tank Tuned Liquid Damper、Vibration Mitigation、Fluid Rotation**

About the Author

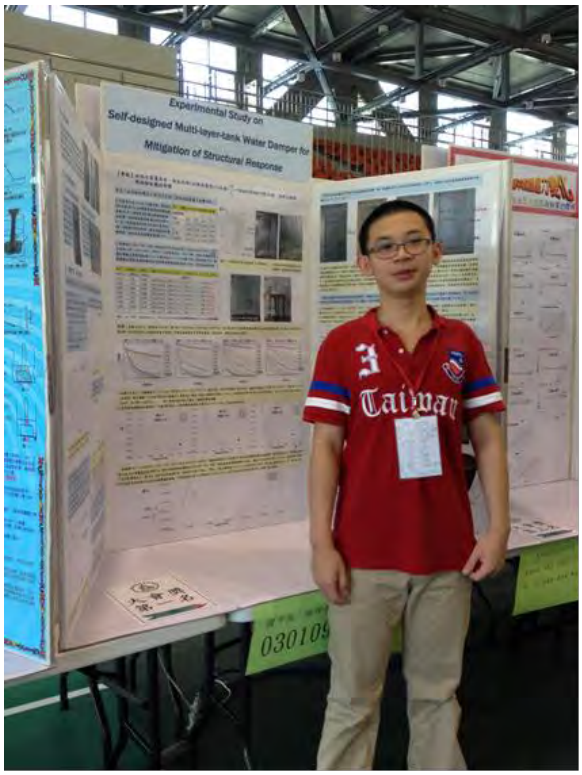

Hi! I’ m Anderson Chen. It’ s the sixth time I participate in science fair. My project is about the paraboloidal tank liquid dampers applied to mitigate the structure vibration during the earthquake. I was originally inspired by the design of Tuned Mass Damper (TMD) in Taipei 101. But I found that if the TMD is replaced by the water tanks with sloshing liquid, as called Tuned Liquid Damper (TLD), can enhance the mitigation of structure vibration for about 50 %. That’ s one of the reason I did this research (but why using paraboloidal tanks, let’ s read the report). Among, I’ ve learnt lots of background knowledge not only in literature reviews and engineering mathematics, but also the analysis of experimental results in Matlab. It also prompted me to think of innovative ways to overcome the difficulties I faced. This kind of problem-based learning helped me learn the correlated knowledge far and wide, which was the most meaningful and interesting part of doing this research. That’ s why I’ m enthusiastic about doing science research. Finally, I want to encourage those who are interested in science to do the project with enthusiasm and persistence, without being affected by traditional education system. I’ m sure you’ ll have lots of acquisition.

摘要

本研究以自製模型模擬「結構物裝設拋物體液槽阻尼器(TLD)」。此 TLD 以多個拋物面容器組成，實驗評估其容器曲率、盛水深、盛水質量比(水質量/總質量)及結構物振幅等參數對減振效應的影響。在不同曲率容器內調整盛水深，使「水體自然擺盪頻率」接近「結構物振動頻率」；水體強烈擺盪時易觀察到水面碎波現象，衍生側向擾動，使水體旋轉，此時「旋轉頻率」亦幾乎等於「結構物振動頻率」，產生更大之共振效應，因此水體可提供較大反向作用力，增加減振效果。結構物振幅越大，水體旋轉可能性越高，減振效應越顯著；增加盛水質量比亦減振效果較佳。但水體旋轉時，結構物亦產生側向位移，因此於容器底部加裝潛沒式導流板，可有效控制液體旋轉方向，使其成對異向旋轉，減低結構物側向位移量。實驗證實藉調整拋物面容器之 TLD 的上述參數，可有效達到減振效果。

Abstract

A series of experiments using homemade model were conducted in this study to simulate the mitigation effects of structure vibration equipped with paraboloidal tank tuned liquid damper (TLD). The TLD was constructed by multiple open paraboloidal tanks filled with water oscillating to and fro to damp the external horizontal excitation in arbitrary directions. By using multiple paraboloidal tanks arranged in a transverse array, the damping effects of structure under the longitudinal vibration were compared for various configurations of tank curvatures, water depths, mass ratios (as water to gross mass) and initial amplitudes of structure vibration. The optimal mitigation effects of structure vibration with TLD were achieved when the water depths inside the specific curvatures of paraboloidal tanks were all tuned up so that the natural sloshing frequency of water coincides with the frequency of structure vibration (near resonant condition). The relatively intense motion of sloshing fluid with breaking wave were observed which pushed the fluid in lateral motion. As the fluid in TLD rotates, its frequency is approximately equals to the vibration frequency of structure. As it reaches the resonant condition, the rotating fluid will generate the larger anti-phase longitudinal forces to mitigate the structure vibration more efficiently. Under these conditions, the larger the excitation amplitude of structure is, the more the possibility of fluid rotation occurred, and the better the mitigation effects of vibration will be achieved. Also, the larger mass ratio of liquid in TLD to structure leads to better mitigation effects of vibration. However, the fluid rotation in TLD will also adversely provoke the lateral displacements of structure. To keep from this adversity, the submerged flow-guiding vanes with certain oblique angle were installed at the bottom of each water tank to control the desired direction of fluid rotation. So that the rotating fluid in a pair of TLD can counteract the lateral applied forces between each other to avoid the lateral displacements of structure. The study illustrated that the paraboloidal tank TLD with paired flow-guiding vanes is a useful damping device applied to mitigate the vibration of structure.

Chapter 1 Introduction

Due to the rapid urbanization, there is an increasing demand of high rise buildings in metropolitan areas. Regarding to safety and serviceability designs under external dynamic loads due to wind action or earthquake, the vibration control of these buildings is one essential factor to be assessed. It thus attracts much attention to find both efficient and economical way to mitigate the vibration as much as possible. In this research, we will carry out the experimental study on the passive damping system constructed by the Tuned Liquid Damper (TLD) consisting of multiple open paraboloidal tanks of the same shape. The examined damping system is first activated by the movement of structure and then generates the reacting forces to suppress the vibration response through the splash of liquid inside the TLD, which dissipates the energy due to different resonant mechanisms. Following are the reviews of various kinds of passive supplemental damping systems which are applied worldwide. We will present some laboratory results for our innovative designs of paraboloidal tank TLD on vibration mitigation.

1.1 Tuned Mass Damper (TMD)

Tuned Mass Damper (TMD) as illustrated in Fig. 1-1 is a kind of damping device, using a massive object with steel hanging cables mounted above and the springs-dashpots-hydraulic cylinders set below to work together as a damped pendulum system, hanging inside a high rise building to absorb its seismic or wind energy of vibration [1][2]. The mitigation effect of structure vibration is achieved by tuning the frequency of the damper movement that equals to the natural frequency of structure vibration. By this way, the anti-resonant condition between the damper and the structure occurs due to the effect of inertia created dynamically by the damper movement. That means the direction of damper movement is approximately anti-phase to the structure vibration, so that the damper provides the opposite damping forces to mitigate the vibration of structure. It's a widely used device at present to mitigate the structure vibration of a high rise building. However, there are some disadvantages in application of TMD [3]:

(1) It needs frictionless rubber bearings, springs, dashpots and other mechanical components which usually increase the cost of device installation and maintenance service.

(2) It needs a large spacing for installation and the dead weight of mass has no other functions except for a damper.

Fig. 1-1 The damping system of Taipei 101 and the device of Tuned Mass Damper (TMD)

Some famous examples of TMD installation on the buildings or structures in practice are listed [2].

Name of Building/ Structure	City/ Country	Operation Year
Citigroup Center	New York/ USA	1977
Yokohama Landmark Tower	Yokohama/ Japan	1993
One Wall Centre	Vancouver/ Canada	2001
Taipei 101	Taipei/ Taiwan	2004
Bloomberg Tower	New York/ USA	2004
Shanghai World Financial Centre	Shanghai/ China	2008
Tokyo Skytree	Tokyo/ Japan	2012

1.2 Tuned Liquid Damper (TLD)

Tuned Liquid damper (TLD) is another form of Tuned Mass Damper, with the massive object replaced by one or more liquid containers (generally filled with water, hence, the words of "water," "liquid" and "fluid" are used interchangeably throughout this study). The liquid movement inside the container is allowable to shift its gross mass center dynamically to response for the vibration of structure [3]. That means the TLD can mitigate the structure vibration via the reacting forces exerted by the sloshing liquid in the container which is approximately anti-phase to the structure vibration due to the effect of inertia created by the liquid movement [4] (see Fig. 1-2). A TLD system is usually implemented as a passive device which can be further divided into two main categories: Tuned Liquid Column Damper (TLCD) and Tuned Liquid Sloshing Damper (TLSD). We will concern about the latter and call it simply as TLD in this study.

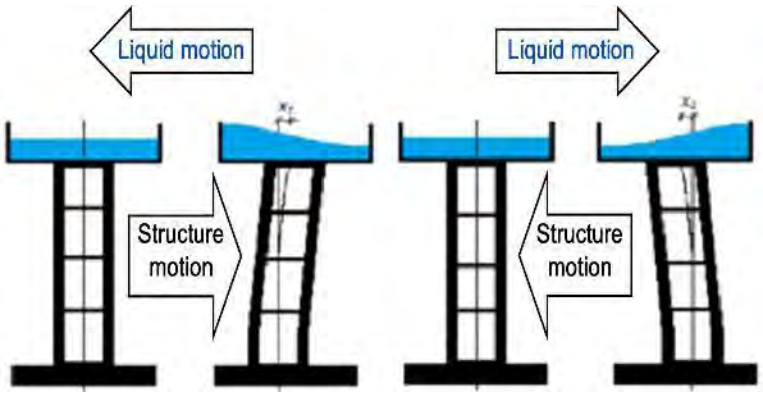

Fig. 1-2 The motion of structure with TLD [4]

The Tuned Liquid Sloshing Damper mitigates the structure vibration via the reacting forces through the sloshing liquid on the tank wall. In addition, the sloshing energy is also dissipated by the liquid friction on the solid boundary or due to the occurrence of breaking wave on the water surface. For the latter, when the wave amplitude reaches a critical value, the overturn or collapse of wave front causes the breaking wave near the wall, as shown in Fig. 1-3. Which will always transform large amounts of wave energy into turbulent kinetic energy and dissipate into thermal energy. At this point, simple linear models are usually not able to describe the large-amplitude

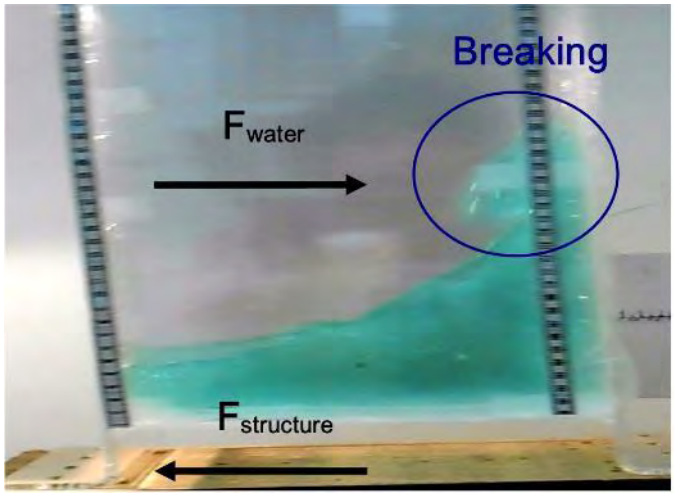

Fig. 1-3 The occurrence of breaking wave in Tuned Liquid damper (TLD)

motion of liquid sloshing and breaking properly [5]. Experimental study is the most convenient way to get complete information of the damping behaviors.

Some of the important TLD parameters were introduced by Banerji et al. (2000) [6] such as the water depth and water mass ratio (as the ratio of water mass to the gross structure) which are confirmed to significantly affect the vibration mitigation of using TLD attached to the structure. Comparing to other kinds of passive mass dampers, the TLD has many advantages [7]:

(1) Easy for installation and maintenance.
(2) Effective in gross cost since the space of water tanks can be combined to the water storage system or the liquid fuel tanks for liquid supply, fire emergency or many other purposes. Without extra loadings applied to the structure with TLD since it is usually a necessity for a structure system.
(3) Easy to tune the effective parameters such as liquid depth or the tank dimensions under different applications.
(4) Allowable to be designed as a multi-directional damper to mitigate the vibration of Multi Degree-of-Freedom (MDOF) structures suffered from wind action and earthquake.
(5) Effective under small-amplitude or large-amplitude vibration.

Fig. 1-4 The combination of structure with Tuned Liquid Damper (TLD)

According to these advantages, TLD has already found in many applications [8], such as satellites (nutation dampers), marine vessels, towers, bridges and tall buildings. Fig. 1-4 shows the schematic application of multi-directional TLD installed on the top of a building in combination with the design of water storage tanks. In the following, some practical examples of buildings or structures with the usage of TLD in civil engineering are listed [4] [7].

Name of Building/ Structure	City/ Country	Shape of TLSD	Operation Year
Nagasaki Airport Tower	Nagasaki, Japan	Circular	1987
Yokohama Marine Tower	Yokohama, Japan	Circular	1987
Gold Tower	Udatsu, Japan	Rectangular (Unidirectional)	1988
Shin Yokohama Prince Hotel	Yokohama, Japan	Circular	1991
Mount Wellington Broadcasting Tower	Hobart, Australia	Circular	1992
TYG Building	Atsugi, Japan	Double donut	1992
Narita Airport Tower	Narita, Japan	Circular	1993
Haneda Airport Tower	Tokyo, Japan	Circular	1993

Chapter 2 Literature Reviews and Study Aims

Since 1980s, many studies on the damping efficiency of various TLD designs have been carried out to find out the effective application in mitigating the seismic and wind vibration of the structure. These researches have mostly focused on the rectangular and cylindrical tank TLD which are first introduced as following.

2.1 Rectangular Tank TLD

As early as the end of 19th century, the liquid waves in an oscillating container were studied and applied [8]. The study continued through the era in development of aerospace vehicle to the present age of modern computer technology. Recently, Bauer (1984 [9]) applied the rectangular tank TLD to control the structure vibration. Since the fast progression of computer technique, numerical models were developed to predict the fluid sloshing motion for rectangular tank TLD. Sun et al. (1991 [10]) introduced the linear shallow water wave theory for the liquid sloshing in rectangular tank. Also, Sun et al. (1992 [11]) developed a nonlinear model for rectangular tank TLD based on the shallow water wave theory in order to introduce the coefficients to account for the effect of breaking wave, which is absence in many other models. Banerji et al. (2000 [6]) studied the effectiveness of some important TLD parameters in rectangular tank based on the model introduced by Sun. The optimum conditions of water depth, water mass ratio (as the ratio of water mass to the gross structure) and fluid sloshing frequency were investigated via the experiments. Also, the designs of TLD were suggested to control the vibration of structure.

2.2 Cylindrical Tank TLD

The rectangular tank TLD can only mitigate the structure response under single direction of excitation, which is a big disadvantage. For improvement, some of the studies as following have been done to investigate the cylindrical tank TLD which can mitigate the structure vibration under multiple directions of excitation:

Wakahara et al. (1992 [12]) and Tamura et al. (1995 [13]) introduced the effectiveness of cylindrical tank TLD applied in real structures, i.e. Nagasaki airport tower, Yokohama Marine tower and Shin Yokohama Prince hotel to mitigate the structural vibration under multiple directions of excitation.

Ibrahim and Li (1988 [14]) suggested the numerical models, including the linear and nonlinear interactions between the fluid sloshing in cylindrical tank to the structure response. Yu (1997 [15]) has researched the cylindrical tank TLD under different conditions of tank diameters and water depths to mitigate the wind-induced vibration. The experiment investigated the fluid sloshing dynamics in cylindrical tank TLD with different water depths. The time history of free water surface oscillation response due to the propagation of standing wave was measured for analysis. Shigehiko and Yasuo (2000 [16]) introduced the linear wave theory applied to the cylindrical tank in order to predict the natural frequency and the time history of the free water surface oscillation

response due to the propagation of standing wave while sloshing. Also, the formulation based on finite amplitude wave theory was used in this study to predict the fluid sloshing dynamics of the cylindrical deep water type TLD.

2.3 Other Tank Geometries of TLD

Except the type of rectangular and cylindrical tank TLD, some of the studies have investigated the effects of sloped-bottom or even the curved-bottom tank TLD as following:
Deng and Tait (2009 [17]) numerically investigated the fluid sloshing dynamics, including the natural frequencies and the effective mass ratios (the percentage of fluid participates in sloshing) of fluid sloshing in the trapezoidal or triangular sloped-bottom tank, and the parabolic curved-bottom tank compared to the rectangular flat-bottom tank by using the linear long wave theory. The research indicated that the parabolic curved-bottom tank provides the highest effective mass ratio while the fluid sloshing. Also, the trapezoidal sloped-bottom tank with a sloping angle of 20 degrees provides the higher effective mass ratio than other sloping angles and the rectangular flat-bottom tank. Which are the effective TLD tank shapes.

Hassan Morsy (2010 [18]) experimentally studied the modified TLD, such as sloped-bottom tank TLD. The results indicated that the sloped-bottom tank TLD is more effective on vibration mitigation than rectangular flat-bottom tank TLD. Also, when the water wave propagates from deep to shallow water zone in the sloped-bottom tank TLD, it will cause the wave shoaling and increase the wave height due to the change of water depth [5] [19]. Which will be more possibility of breaking wave phenomenon occurred and dissipate the energy.

2.4 Study Aims

In this study, we will concentrate only on the damping effects of structure vibration by the usage of paraboloidal tank TLD (Fig. 2-1), which has some advantages according to the literature reviews above. Those are summarized as following:

1. It can mitigate the vibration of structure under multiple directions of excitation.
2. It has a curved bottom, due to the change of water depth, it may cause the wave shoaling during the propagation of water wave. Which will be more possibility of breaking wave phenomenon occurred and dissipate the energy.
3. The numerical study suggested by Deng and Tait (2009 [17]) indicated that the TLD water tanks with sloped and curved bottom can provide the higher effective mass ratios while the fluid sloshing. Which may be more effective on vibration mitigation.

So, the aims of this study are as following:

1. To Evaluate the Effects of **Curvatures** of Paraboloidal Tank TLD on Vibration Mitigation.
2. To Evaluate the Effects of **Water Depths** (The Water Surface Level is **Below, Above or Exactly on the Focal Plane**) of Paraboloidal Tank TLD on Vibration Mitigation.

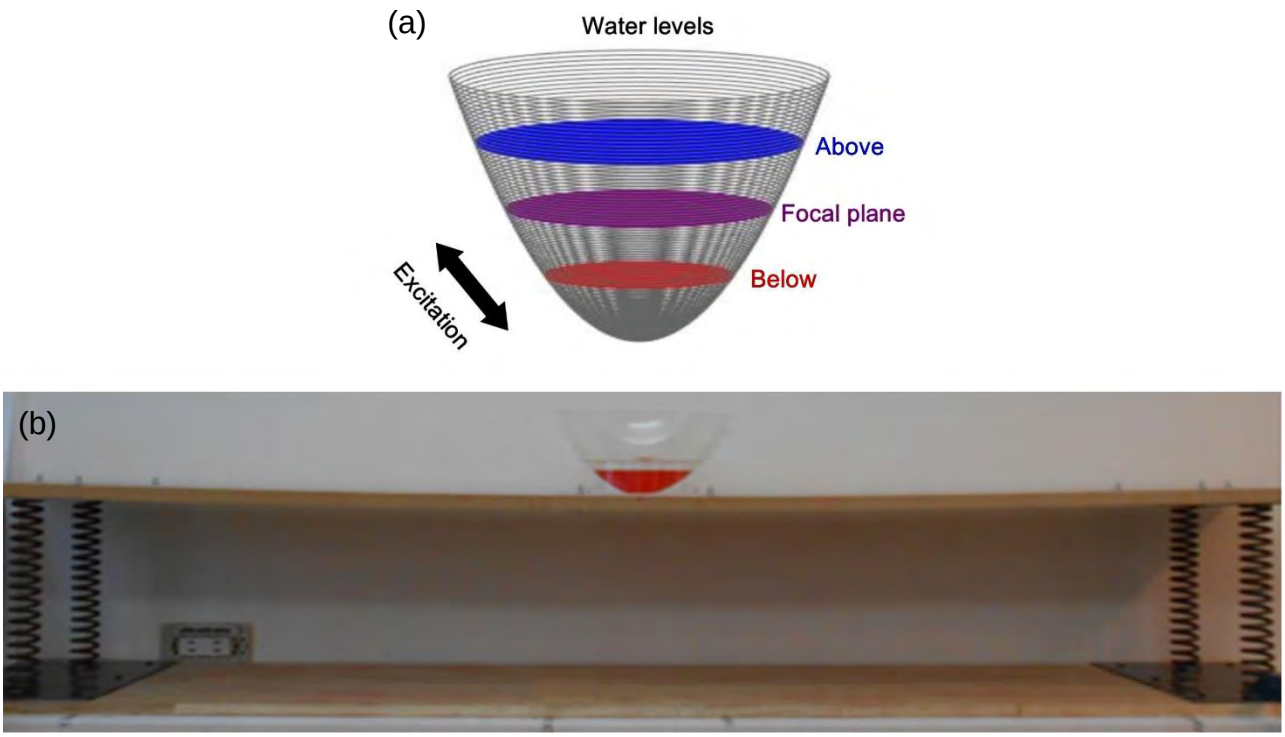

Fig. 2-1 (a) The shape of paraboloidal tank (b) The structure with a paraboloidal tank TLD

Chapter 3 Theoretical Backgrounds

3.1 The Fluid Sloshing Dynamics in the Paraboloidal Tank (Rigid Containers)

Bauer(1984 [20], 1999 [21]) used the paraboloid coordinate surfaces as the boundaries to approximate the liquid motion of the free surface splashing in the paraboloidal tank. The coordinate system (ξ, η, φ) as shown in Fig. 3-1 are utilized to get the analytic solutions. Here the related linear theory is briefly summarized, according to Ibrahim (2005 [8]).

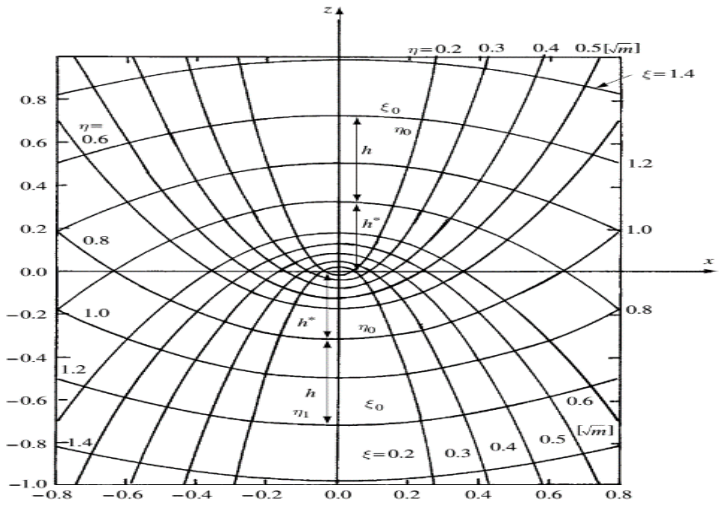

Fig. 3-1 Paraboloid coordinate system in the plane of φ = 0

The shape of container wall, $\eta = \eta_0$, satisfies exactly the equation

$$z = -\frac{\eta_0^2}{2} + \frac{1}{2\eta_0^2}(x^2 + y^2) \tag{3.1}$$

while the flat free surface approximately matches the coordinate line $\xi = \xi_0$ as

$$z = \frac{\xi_0^2}{2} - \frac{1}{2\xi_0^2}(x^2 + y^2) \tag{3.2}$$

or, the approximate location

$$z = \frac{\xi_0^2}{2} - \frac{\eta^2}{2}\ , 0 \le \eta \le \eta_0 \tag{3.3}$$

for $\xi_0 >> 1$. With these geometry equations of boundary, the flow equations governed by Laplace's equation and the boundary conditions are written in the paraboloid coordinates

$$\frac{\partial^2\Phi}{\partial\xi^2} + \frac{1}{\xi}\frac{\partial\Phi}{\partial\xi} + \frac{\partial^2\Phi}{\partial\eta^2} + \frac{1}{\eta}\frac{\partial\Phi}{\partial\eta} + \frac{(\xi^2+\eta^2)}{\xi^2\eta^2}\frac{\partial^2\Phi}{\partial\varphi^2} = 0 \tag{3.4a}$$

$$\frac{\partial\Phi}{\partial\eta} = 0 \qquad \text{at the side wall } \eta = \eta_0 \tag{3.4b}$$

$$\frac{\partial^2\Phi}{\partial t^2} + g\frac{1}{\xi}\frac{\partial\Phi}{\partial\xi} = 0 \qquad \text{at the free surface } \xi = \xi_0 \tag{3.4c}$$

where Equation (3.4c) represents the linearized free-surface condition. The Fourier series solution of Equation (3.4a) that satisfies the wall boundary condition (3.4b) is

$$\Phi\,(\xi,\eta,\varphi,\mathrm{t}) = \sum_{m=0}^{\infty}\sum_{n=1}^{\infty} A_{mn}\, I_m\left(\frac{\varepsilon_{mn}\xi}{\eta_0}\right) J_m\left(\frac{\varepsilon_{mn}\eta}{\eta_0}\right)\cos(m\varphi)\; e^{i\omega t} \tag{3.5}$$

where J_{m} and I_{m} are the Bessel function and its modified one of the first kind of m$^{\mathrm{th}}$-order (ε_{mn} are the zeros of J'_m). Substituting (3.5) into (3.4c) gives the natural frequency of the free surface

$$\omega_{mn}^2 = \frac{g\varepsilon_{mn}}{\xi_0\eta_0}\frac{I'_m(\frac{\varepsilon_{mn}\xi_0}{\eta_0})}{I_m(\frac{\varepsilon_{mn}\xi_0}{\eta_0})} \tag{3.6}$$

With the lowest mode m = n = 1 we have the fundamental frequency of water sloshing. The Fourier coefficients A_{mn} in (3.5) are necessarily determined further by the external forcing condition. Under a sinusoidal excitation in the x-direction, $x(t) = X_0 e^{i\Omega t}$, the velocity potential has the form $\Phi(\xi,\eta,\varphi,\mathrm{t}) = \{\mathrm{i}\Omega X_0\xi\eta + \widetilde{\Phi}(\xi,\eta)\}\cos\varphi\, e^{i\Omega t}$, where the perturbed function $\widetilde{\Phi}$ satisfies the boundary condition

$$\frac{\partial\widetilde{\Phi}}{\partial\eta} = 0, \quad at\ \eta = \eta_0 \tag{3.7}$$

Finally, the solution of velocity potential function for a sinusoidal excitation in a paraboloid tank is

$$\Phi\,(\xi,\eta,\varphi,t) = \left\{i\Omega X_0\xi\eta + \sum_{n=1}^{\infty} A_{1n}\, I_1\left(\frac{\varepsilon_{1n}\xi}{\eta_0}\right) J_1\left(\frac{\varepsilon_{1n}\eta}{\eta_0}\right)\right\} cos\varphi\; e^{i\Omega t} \tag{3.8}$$

with the coefficient A_{1n} given by

$$A_{1n} = i\frac{2\Omega X_0(\Omega^2\xi_0^2 - g)\,\eta_0}{\xi_0(\omega_{1n}^2-\Omega^2)(\varepsilon_{1n}^2-1)J_1(\varepsilon_{1n})I_1\left(\frac{\varepsilon_{1n}\xi_0}{\eta_0}\right)} \tag{3.9}$$

From this solution, the square of the natural frequency of the surface is

$$\omega_{1n}^2 = \frac{g\varepsilon_{1n}}{\xi_0\eta_0}\frac{I'_1(\frac{\varepsilon_{1n}\xi_0}{\eta_0})}{I_1(\frac{\varepsilon_{1n}\xi_0}{\eta_0})} \tag{3.10}$$

Accordingly, the free-surface wave height is

$$z = -\frac{1}{g}\frac{\partial\Phi}{\partial t}\Big|_{\xi=\xi_0} = \Omega^2\frac{X_0}{g}\left\{\xi_0\eta + 2\sum_{n=1}^{\infty}\frac{(\Omega^2\,\xi_0 - \frac{g}{\xi_0})\eta_0\, J_1\left(\frac{\varepsilon_{1n}\eta}{\eta_0}\right)}{(\omega_{1n}^2-\Omega^2)(\varepsilon_{1n}^2-1)J_1(\varepsilon_{1n})}\right\}\cos\varphi\; e^{i\Omega t} \tag{3.11}$$

and the pressure distribution is

$$p = \rho\Omega^2 X_0\left\{\xi\eta + 2\eta_0\sum_{n=1}^{\infty}\frac{(\Omega^2\,\xi_0 - \frac{g}{\xi_0})I_1\left(\frac{\varepsilon_{1n}\xi}{\eta_0}\right)J_1\left(\frac{\varepsilon_{1n}\eta}{\eta_0}\right)}{(\omega_{1n}^2-\Omega^2)(\varepsilon_{1n}^2-1)J_1(\varepsilon_{1n})I_1\left(\frac{\varepsilon_{1n}\,\xi_0}{\eta_0}\right)}\right\} cos\varphi\; e^{i\Omega t} + \frac{\rho g(\xi_0^2-\xi^2)}{2} \tag{3.12}$$

Therefore, the hydrodynamic force is obtained by integrating the pressure over the wetted area

$$F_x = m\Omega^2 X_0\frac{\xi_0^2}{\xi_0^2+\eta_0^2}\left\{1 + 8\frac{\eta_0}{\xi_0}\sum_{n=1}^{\infty}\frac{(\Omega^2 - \frac{g}{\xi_0^2})I_2\left(\frac{\varepsilon_{1n}\xi}{\eta_0}\right)}{\varepsilon_{1n}(\omega_{1n}^2-\Omega^2)(\varepsilon_{1n}^2-1)I_1\left(\frac{\varepsilon_{1n}\,\xi_0}{\eta_0}\right)}\right\} e^{i\Omega t} \tag{3.13}$$

3.2 The Mean Curvature of Paraboloidal Surface

Let p be a point on the surface S. A signed curvature is defined by the intersection curve of the surface S with a plane through p containing the normal line to S. As this plane is rotated around the normal line, the curvature varies and we then have the maximal curvature κ_1 and minimal curvature κ_2 known as the principal curvatures of S. Taking the average of the principal curvatures leads to the **mean curvature** [22]

$$H = \frac{1}{2}(\kappa 1 + \kappa 2) \tag{3.14}$$

For the surface defined as a function of two coordinates, $z = S(x, y)$, the mean curvature *H* can be expressed in

$$2H = \nabla \cdot \left(\frac{\nabla S}{\sqrt{1+|\nabla s|^2}}\right) = \frac{(1+\left(\frac{\partial S}{\partial x}\right)^2)\frac{\partial^2 S}{\partial y^2}+(1+\left(\frac{\partial S}{\partial y}\right)^2)\frac{\partial^2 S}{\partial x^2}-2\frac{\partial S \partial S}{\partial x \partial y}\frac{\partial^2 S}{\partial x \partial y}}{(1+(\frac{\partial S}{\partial x})^2+ (\frac{\partial S}{\partial y})^2)^{\frac{3}{2}}} \tag{3.15}$$

According to the definition as Equation (3.15), the mean curvature *H* of the paraboloidal surface

$$z = S(x, y) = \frac{x^2+y^2}{4p} \tag{3.16}$$

where z is the height and p is the vertical distance from vertex to focal plane of paraboloidal tank. Substituting (3.16) into (3.15), the mean curvature becomes

$$H = \frac{2+\frac{z}{p}}{4p\left(1+\frac{z}{p}\right)^{\frac{3}{2}}} \tag{3.17}$$

In this study, the heights of the paraboloidal tanks (z) were constantly 12 cm (Chapter 4). So, the smaller the value of p, the larger the mean curvature of the paraboloidal tank.

Chapter 4 Experiment Setup & Analysis

4.1 Methodology

As shown in Fig. 4-1, four stiff steel springs of 25 cm in length and 3.6 cm in diameter, rigidly founded by two thin metal plates of 0.3 cm thick fixed on the floor, supported on both sides of horizontal plates made of rectangular wooden boards of 1.8 cm thick. This simple structure model allows to vibrate horizontally in order to simulate the motion of a multistory shear building supported by four columns. Also, an array of open paraboloidal tanks, made of Plexiglas acrylic sheet, which were filled partially with water and firmly attached to the plate top, formed a TLD model installed on the top of the structure. The system of structure accompanied with an array of TLD water tanks which was initially displaced by a required distance and set free later on to vibrate horizontally in the experiment to study the horizontal vibration behaviors of structure with liquid dampers. To confirm the validity of only horizontal motion of structure to be considered, the maximum vertical displacement of negligible amount of 0.3 cm was found for the extreme case of structure vibration. Therefore, the experiments omitted the effects from vertical vibration.

Fig. 4-1 A paraboloidal tank TLD installed on the top of the structure

The homemade paraboloidal tanks of 12 cm in heights distinguished from six different mean curvatures (H) as Tank A to F in Fig. 4-2 were utilized as elements of TLD system. The details of the designs of water tanks with the verification of accuracy are all illustrated in Appendix 1.

All tested cases setup for various TLD parameters in this study as shown in Table 4-1. Among these, six different curvatures of paraboloidal tanks are recognized as Tank A to F. Three different water surface levels in TLD were set up respectively as *below*, *exactly on* or *above* the focal plane of paraboloidal tanks. Hence, the total volumes of water in the experiment groups were controlled all equally as 90, 120, 180 ml, which are corresponding to three setup mass ratios of water to the gross mass of structure as 0.76 %, 1.01 %, and 1.51 % respectively. To this end, the amount of water tanks filled with water needs to be adjusted. So that the multiple paraboloidal tanks from Tank A to F have the same total weights of 2.76 kgw respectively when they were arranged in an array on the structure transverse to the direction of vibration, as illustrated in Fig. 4-3. The initial setup excitation amplitudes of structure were 1, 2, 3 cm respectively. For reproducibility, each case was repeated for five times. Meanwhile, the trajectory of a small spherical submerged particle of 3.44 g/ cm^3 in density and 0.55 cm in diameter was traced along the tank wall (as seen in Fig. 4-4) to clarify the fluid sloshing dynamics of TLD during the vibration of structure.

Fig. 4-2 Six different curvatures (H = 0.044~0.061) of paraboloidal tanks (Tank A to F)

Table 4-1 The Setup TLD Parameters

Tanks			A	B	C	D	E	F
Mean Curvatures (1/cm)			0.044	0.049	0.053	0.055	0.058	0.061
Water Depths (cm)	Below Focal Plane		2.16	1.72	1.50	1.36	1.19	1.08
	Exactly On Focal Plane		3.06	2.43	2.12	1.93	1.68	1.53
	Above Focal plane		4.33	3.44	3.00	2.73	2.38	2.16
Volume of Water **Per Tank** (ml)	Below Focal Plane (=0.5V)		90	45	30	22.5	15	11.25
	Exactly On Focal Plane (=V)		180	90	60	45	30	22.5
	Above Focal plane (=2V)		–*	180	120	90	60	45
Amount of Water Tanks Filled with Water	Below Focal Plane	180 ml	2	4	6	8	–	–
		120 ml	–*	–	4	–	8	–
		90 ml	–	2	–	4	6	8
	Exactly On Focal Plane	180 ml	1	2	3	4	6	8
		120 ml	–	–	2	–	4	–
		90 ml	–	1	–	2	3	4
	Above Focal plane	180 ml	–	1	–	2	3	4
		120 ml	–	–	1	–	2	–
		90 ml	–	–	–	1	–	2
Total Amount of Water Tanks			2	4	6	8	8	8

* – : unavailable case in experiment

V= water volume per tank when the water surface level is set up exactly on the focal plane

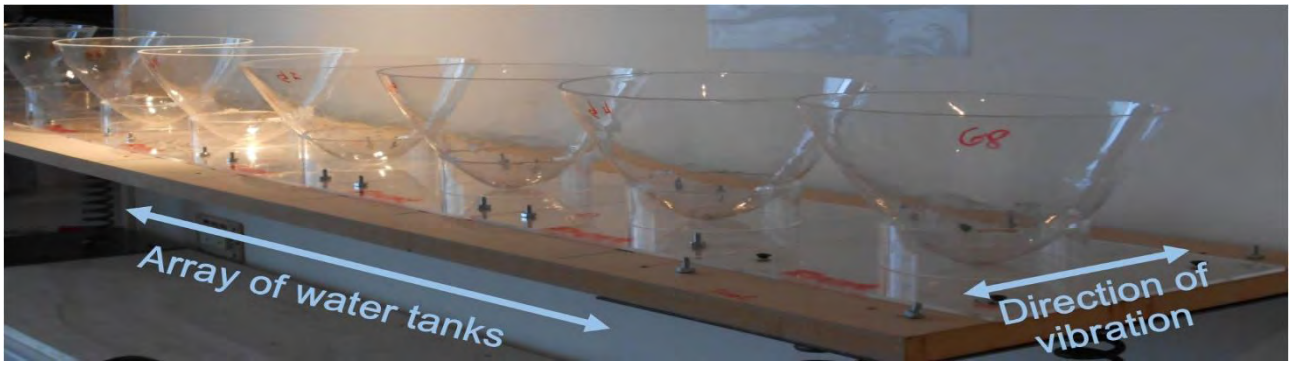

Fig. 4-3 Array of water tanks on the structure transverse to the direction of vibration

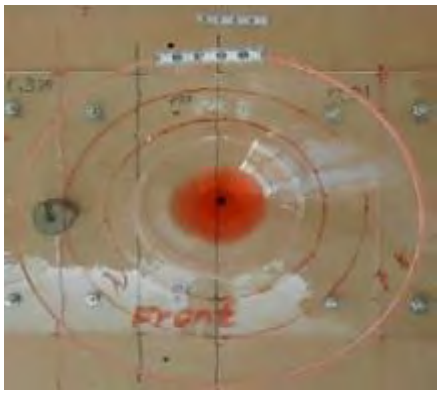

Fig. 4-4 The particle sank inside the water of TLD

4.2 To Analyze the Mitigation Effects of Structure Vibration

The vibration of structure with TLD was recorded by video whose images files were imported into "Tracker" for analysis at a sampling frequency of 30 frames/sec. The evolved displacement $x(t)$ of structure vibration within first 10 seconds is plotted as the blue line in Fig. 4-5. It shows that the envelope of vibration curve (red dashed line) decays exponentially over time, which can be expressed as

$$x(t) = A_0 e^{-ct} \qquad (4.1)$$

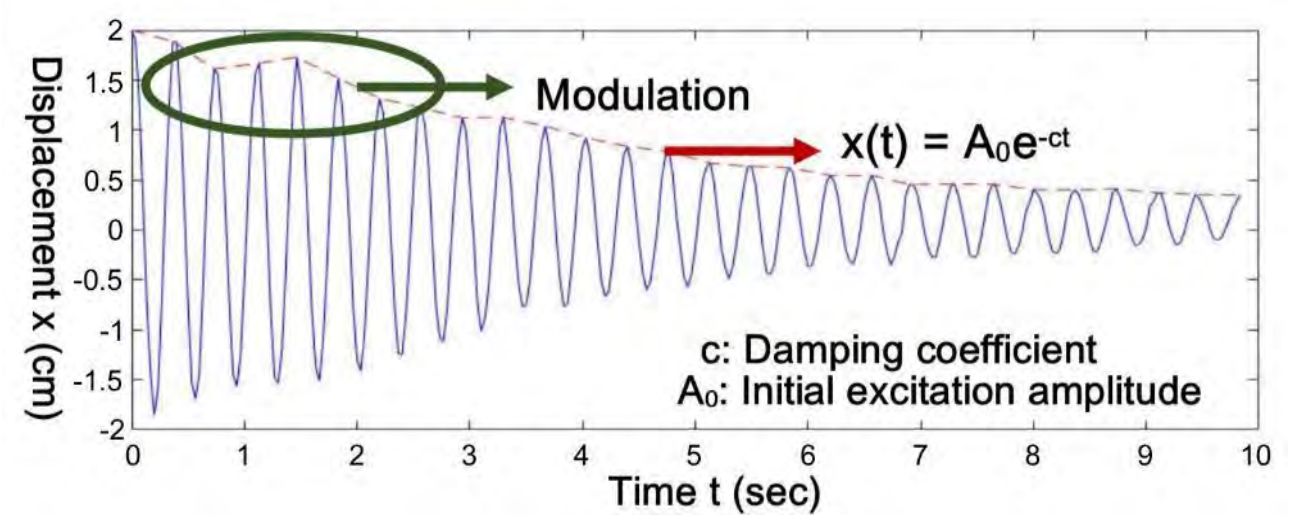

Fig. 4-5 Structure vibration curve

in which the damping coefficient c can quantify the effects of vibration mitigation. One also observed in this figure that the modulation of envelop appears within first six setup periods during the vibration of structure with TLD. This makes difficulties to estimate the accurate effects of vibration mitigation by using TLD.

In order to quantify the effects of vibration mitigation more accurately, the Continuous Wavelet Transform (CWT) of the vibration curve was performed in Matlab, whose codes are shown in Appendix 2. Using this transformation enables to decompose the displacement signal *x*(t) from time t-domain into time-frequency (t, f)-domain. In this study, the mother wavelet function of Morlet φ (t) as shown in Fig. 4-6 is specified by

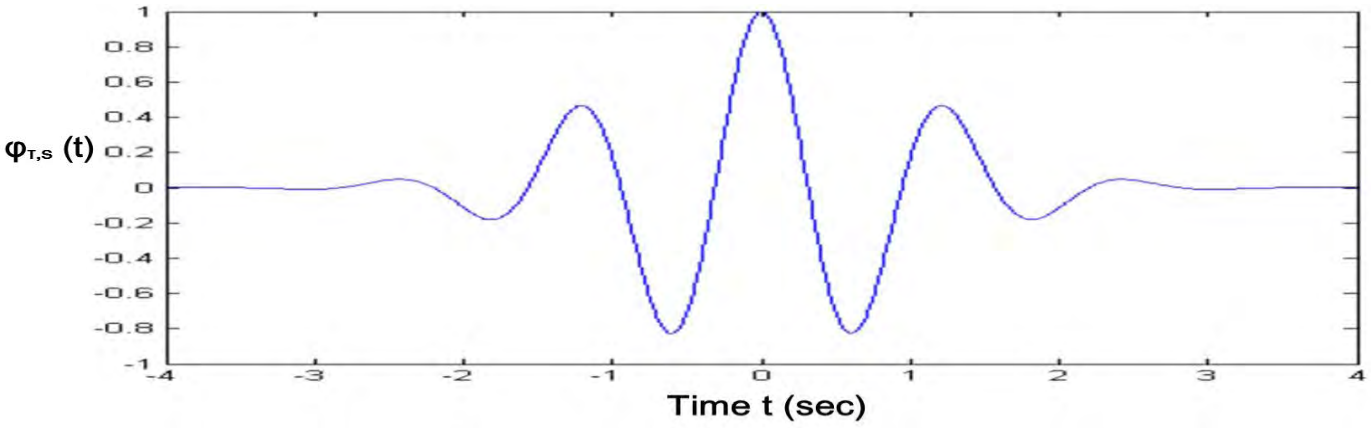

Fig. 4-6 Morlet wavelet function

$$\varphi_{\tau,s}(t) = \frac{1}{\sqrt{s}}\,\varphi\left(\frac{t-\tau}{s}\right), \qquad \tau, s \in R^{+} \tag{4.2}$$

where the operation of dilation is denoted by s and that of translation by τ. Therefore, in the time domain, $\varphi_{\tau,s}$ is centered at τ with a spread proportional to s. The CWT of the vibration curve *x*(t) is defined as

$$\mathrm{CWT}\{x(t)\} = W_x(\tau, s) = \frac{1}{\sqrt{s}}\int_{-\infty}^{\infty} x(t)\varphi^{*}\left(\frac{t-\tau}{s}\right)\,dt \tag{4.3a}$$

in which φ^{*} is the complex conjugate of the wavelet function φ. The wavelet coefficient $W_x(\tau, s)$ in (4.3a) measures the variation of the vibration curve x(t) in the neighborhood of position τ. By varying the scale s and translating along the localized time τ, the wavelet modulus $|W_x(\tau, s)|$ can construct a wavelet plot after transforming the scale (s) to frequency (f) as following

$$f = \frac{f_c}{s} \tag{4.3b}$$

where f_c is the central frequency (resolution) of wavelet. That shows the amplitude of the feature in the vibration curve against the scale and how the amplitude varies with time under different frequencies conditions. Therefore, the information in the time domain will still remain, compares to the Fourier Transform, the time domain information becomes almost invisible. Fig. 4-7 shows a three-dimensional wavelet plot of the structure vibration curve *x*(t) in Fig. 4-5, acquired the amplitude of wavelet modulus $|W_x(t, f)|$ against time (t) and frequency (f). Apparently, the singlet peak in the wavelet plot occurred at the frequency f = fs (within the blue circle in the figure), which is right the fundamental frequency of structure vibration.

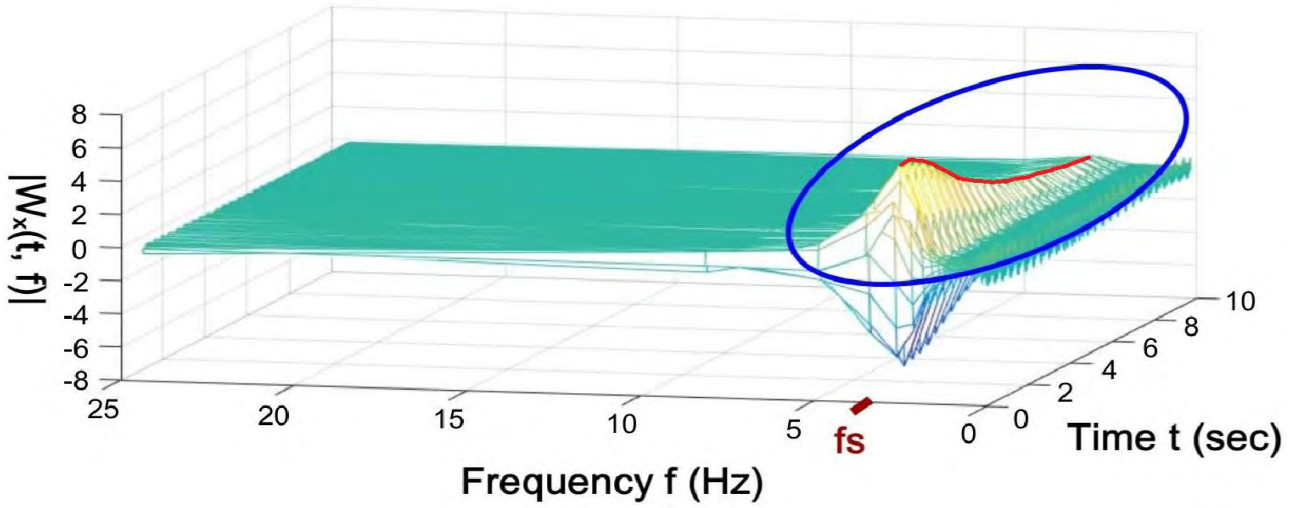

Fig. 4-7 The wavelet plot of the structure vibration curve *x*(t) in Fig. 4-5

The wavelet modulus $|W_x(t, f)|$ can be extracted further from the wavelet plot in Fig. 4-8 at fs, which represents the desired non-modulated vibration curve decomposed from the origin modulated one in Fig. 4-5. After fitting its envelope (blue dots) in red line according to Equation (4.1), we got

$$x'(t) = 7.922e^{-0.241t} \quad (4.4)$$

The estimated damping coefficient (c) = 0.241 can therefore quantify the mitigation effects of structure vibration with the usage of TLD. In practice, the larger the damping coefficient (c) is, the better the mitigation effect of structure vibration is achieved.

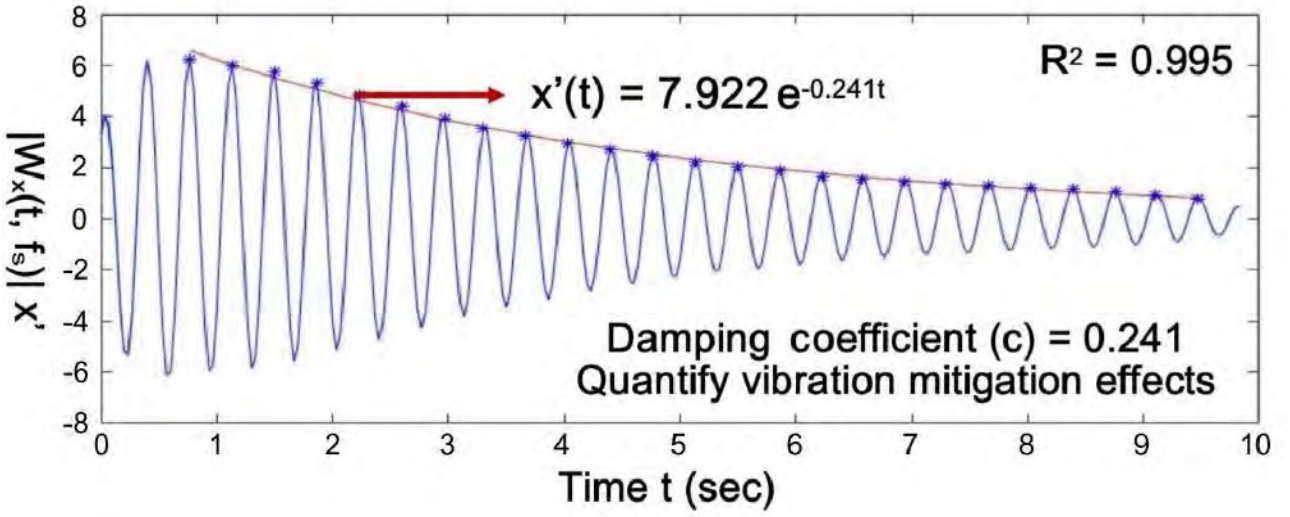

Fig. 4-8 Extracted wavelet modulus from Fig. 4-7 at fs

4.3 To Analyze the Fluid Sloshing Dynamics in TLD

As mentioned in Sec. 4.1, during the water sloshing inside the TLD, the trajectory of a submerged particle moving along the tank wall was also recorded by a video camera fixed above the model. The images files were imported into “Tracker” to digitize the path for first 5 seconds in the space coordinate (x, y, z) (Fig. 4-9), in order to quantify the fluid sloshing dynamics in TLD. To

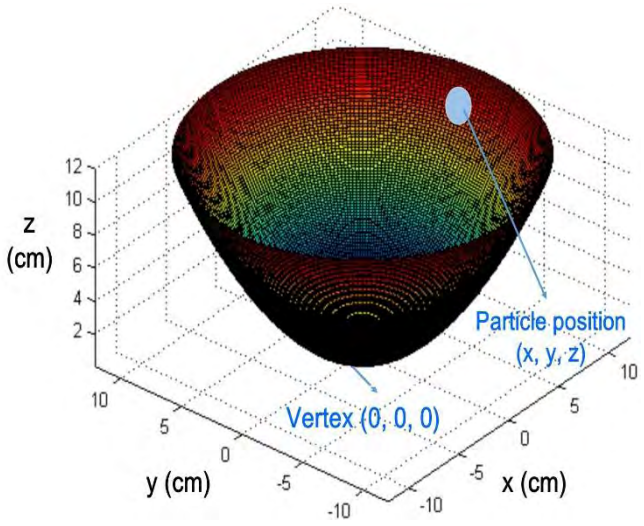

Fig. 4-9 The particle in space coordinate

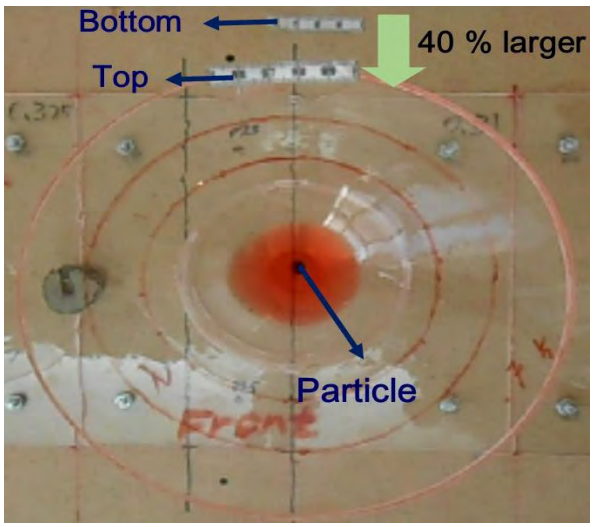

Fig. 4-10 The perspective error of image

correct the perspective error of camera, the justification was related to the z-levels or the vertical locations of particle along the tank bottom. This correction step is essential because it can be deviated much even for the same displacement located at different z-levels. For example, 40 % larger value was found on the top of water tanks (where z = 12 cm) than at the bottom (where z = 0 cm) due to the deviation of perspective view, as illustrated in Fig. 4-10. Therefore, the measured displacement data of particle at certain z-levels in tanks need to be corrected. Two correction steps were done as following:

(1) Two rulers were fixed on two different z-levels, one at the level of tank bottom and another on the top. The percentage of perspective error (D) from the bottom level to the top can be evaluated from the images by both readings of ruler scales in "Tracker".

(2) The ruler at the bottom level was treated as the standard unit of distance in the images as seen in Fig. 4-11. The measured particle displacements at certain z- levels can be corrected by

$$\mathrm{r} = \frac{r_m}{1+z\cdot\frac{D}{H}} \tag{4.5}$$

where

r = **real** distance from the central z-axis to the particle ($r^2 = x^2 + y^2$, referred to Fig. 4-11);

r_m=**measured** distance from the central z-axis to the particle ($r_m^2 = x_m^2 + y_m^2$);

z = z- level of particle on the tank wall;

D = percentage of perspective error from the tank bottom to the top;

H = height of water tank (=12 cm)

Because the particle always moves around the tank wall as $z = r^2/4p$ (where p = vertical distance from vertex to focal plane of paraboloidal tank) during the water sloshing, as seen in Fig. 4-12. Equation (4.5) can change the form as

$$2\sqrt{pz} = \frac{r_m}{1+z\cdot\frac{D}{H}} \tag{4.6}$$

That is, represented for the polynomial of $\sqrt{z}$ as

$$2\sqrt{p}\frac{D}{H}\cdot z^{1.5} + 2\sqrt{p}\cdot z^{0.5} - r_m = 0 \tag{4.7}$$

Solving this by Matlab (using symbolic math toolbox with the codes shown in Appendix 2) for z gives

$$z = \sqrt{\sqrt[3]{\sqrt{\frac{37}{999(\frac{D}{H})^3} + \frac{0.25 \cdot {r_m}^2}{(\frac{D}{H})^2 \cdot (2\sqrt{p})^2}} + \frac{0.5 * r_m}{2\sqrt{p}\frac{D}{H}}} - \frac{1}{3 \cdot \frac{D}{H} \cdot \sqrt[3]{\sqrt{\frac{37}{999(\frac{D}{H})^3} + \frac{0.25 \cdot {r_m}^2}{(\frac{D}{H})^2 \cdot (2\sqrt{p})^2}} + \frac{0.5 * r_m}{2\sqrt{p}\frac{D}{H}}}}} \qquad (4.8)$$

Substituting (4.8) into (4.5), one corrects the measured displacements of particle at certain z- levels in the space coordinate (x, y, z) as shown in Fig. 4-11. By this procedure, the trajectory of the particle motion (x, y, z) can be animated by Matlab. The results are presented in Chapter 5 and the Matlab codes are shown in Appendix 2.

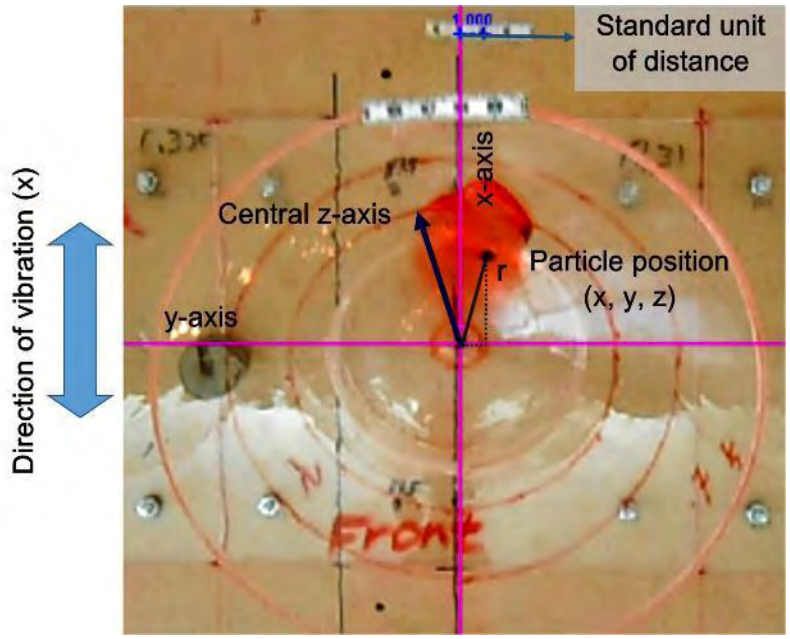

Fig. 4-11 Perspective error correction of particle displacements

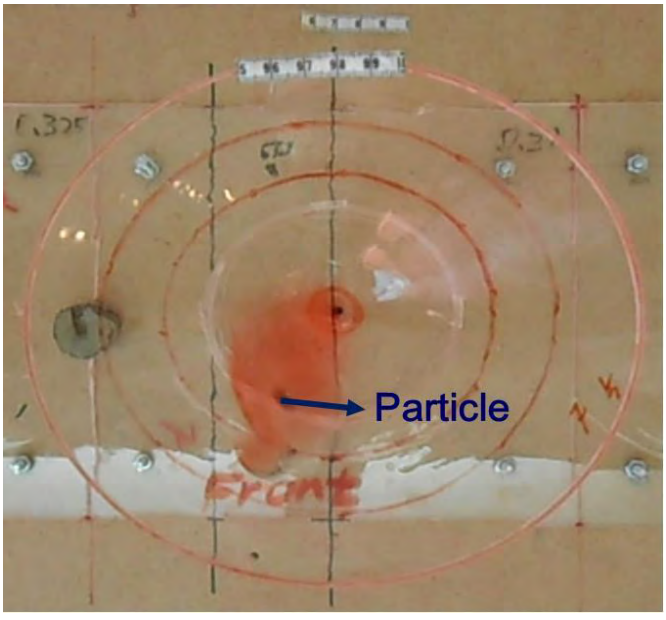

Fig. 4-12 Particle movement around the tank wall while the fluid sloshing

Chapter 5 Experimental Results and Discussion

The experiments evaluated the mitigation effects of structure vibration with paraboloidal tank TLD under six different tank curvatures conditions (of values from 0.044 to 0.061 for Tank A to F), three water depths (the water surface level was below, exactly on or above the focal plane) and three water mass ratios (of 0.76%, 1.01% and 1.51 %), see Table 4.1. The setup initial excitation amplitudes of structure were 1, 2, 3 cm respectively. And the descriptions of fluid sloshing dynamics in TLD were also recorded. The experimental results are summarized as following:

1. Video 5-1 to 5-6 show the animations of the trajectories of particle motion in Tank A to F during the water sloshing in TLD. Fig. 5-1 (a) to (d) show the images of water sloshing in Tank A to D without breaking wave observed. On the other hand, Fig. 5-2 (a) and (b) show that in Tank E and F with the occurrence of breaking wave for first two seconds. All in the cases of water surface levels were set up exactly on the focal plane of paraboloidal tanks and mass ratio = 1.51 % under the initial excitation amplitude of 2 cm.

   Situation 1: In Tank A to D (Video 5-1 to 5-4), the particle inside the water tanks only moved to and fro in the direction of structure vibration. The images of water sloshing are shown in Fig. 5-1 (a) to (d).

5-1: Tank A.mp4 5-2: Tank B.mp4 5-3: Tank C.mp4 5-4: Tank D.mp4

Video 5-1 to 5-4 Trajectories of particle motion in Tank A to D during the water sloshing

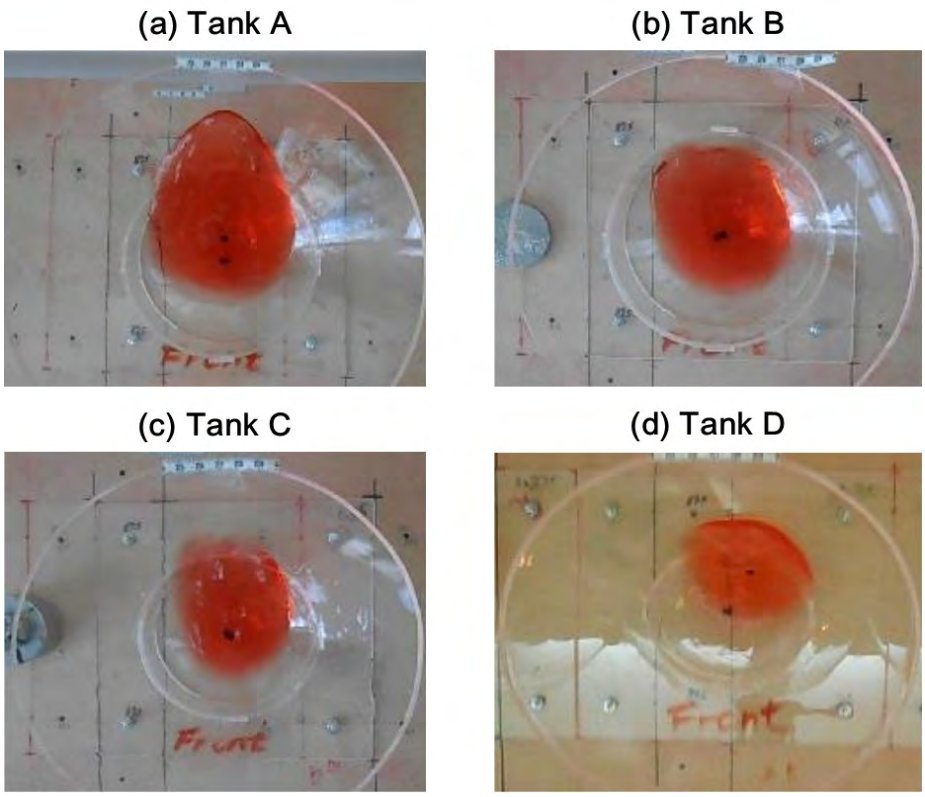

Fig. 5-1 (a) to (d) Fluid sloshing dynamics in Tank A to D (without breaking wave observed)

Situation 2: In Tank E and F (Video 5-5 and 5-6), the particle inside the water also moved to and fro in the direction of structure vibration within first 2 seconds. Then, the breaking wave was observed, as shown in Fig. 5-2 (a) and (b). Meanwhile, the water started to rotate around the tank wall of TLD (Video 5-5 and 5-6), as shown in Fig. 5-3 (a) and (b).

5-5: Tank E.mp4 5-6: Tank F.mp4

Video 5-5 to 5-6 Trajectories of particle motion in Tank E and F during the water sloshing

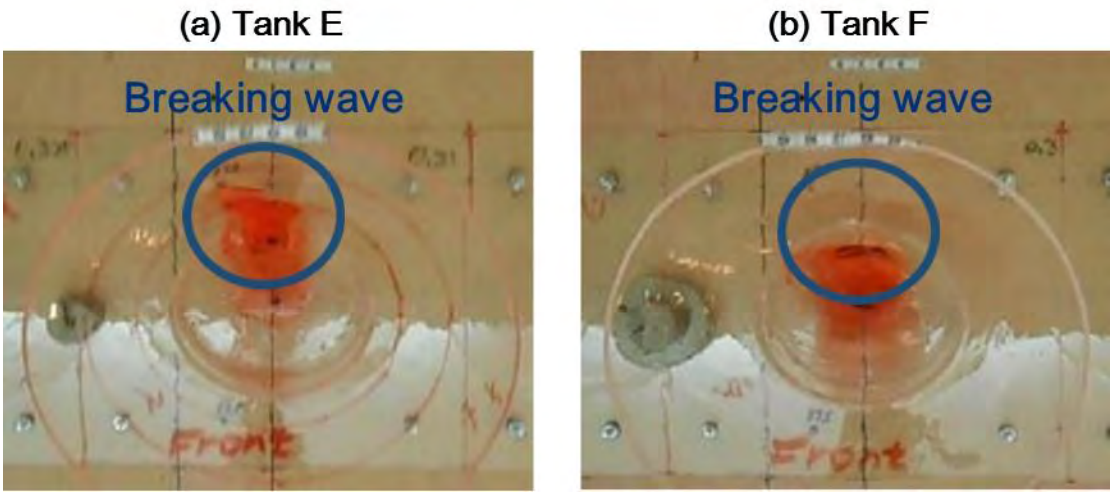

Fig. 5-2 (a) to (b) Water sloshing in Tank E and F with initiate breaking wave (within the blue circle) observed within first two seconds

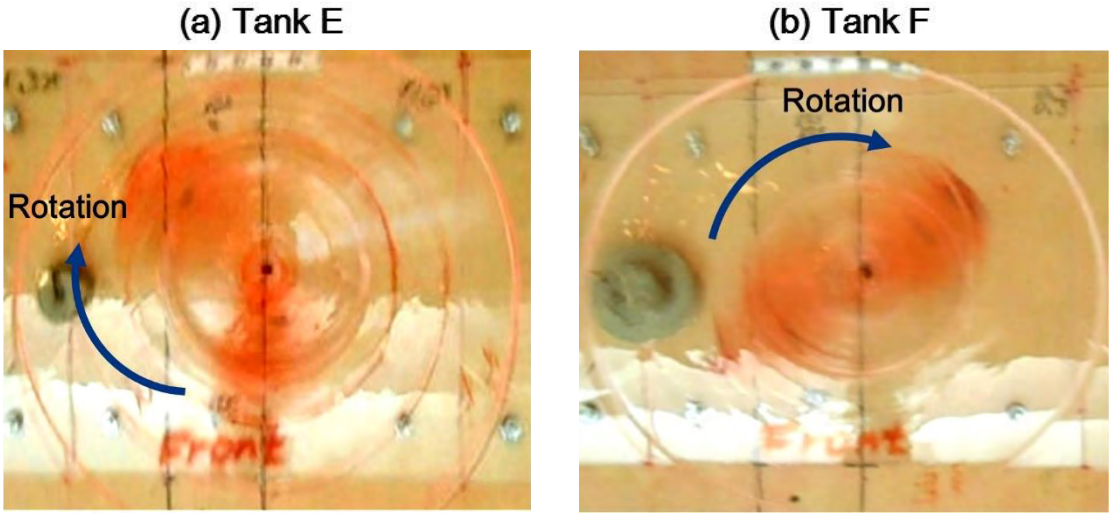

Fig. 5-3 (a) to (b) Water rotates in Tank E and F after the occurrence of breaking wave

2. The mitigation effects of structure vibration with TLD were assessed by the damping coefficient (c) for Tank A to F in Fig. 5-4 to Fig. 5-6. In some cases the fluid rotation in TLD occurred are marked by ★ in these figures. The details of the experimental results are shown in Appendix 3.

(1) Comparing for various tank curvatures utilized, when the water surface level is set up below the focal plane, the optimal mitigation effects of structure vibration appeared for the largest damping coefficient (c) in using Tank E. When the water surface level is set up exactly on or above the focal plane, the optimal mitigation effects of vibration occurred in using Tank F. The fluid rotation in TLD occurred only in the groups of using Tank E and F (marked by ★), the better mitigation effects of vibration occurred under these conditions.

(2) As for various setup water levels, when the water surface level is set up below the focal plane, the better mitigation effects of vibration occurred in using Tank A to E. Conversely, in using Tank F, the better mitigation effects of vibration occurred when the water surface level is setup exactly on the focal plane.

(3) As for various water mass ratios of TLD and the initial excitation amplitudes of structure, the better mitigation effects of vibration were always achieved for both having larger setup values. Moreover, in using Tank E and F, the larger the initial excitation amplitude of structure was, the more the possibility of fluid rotation in TLD was observed.

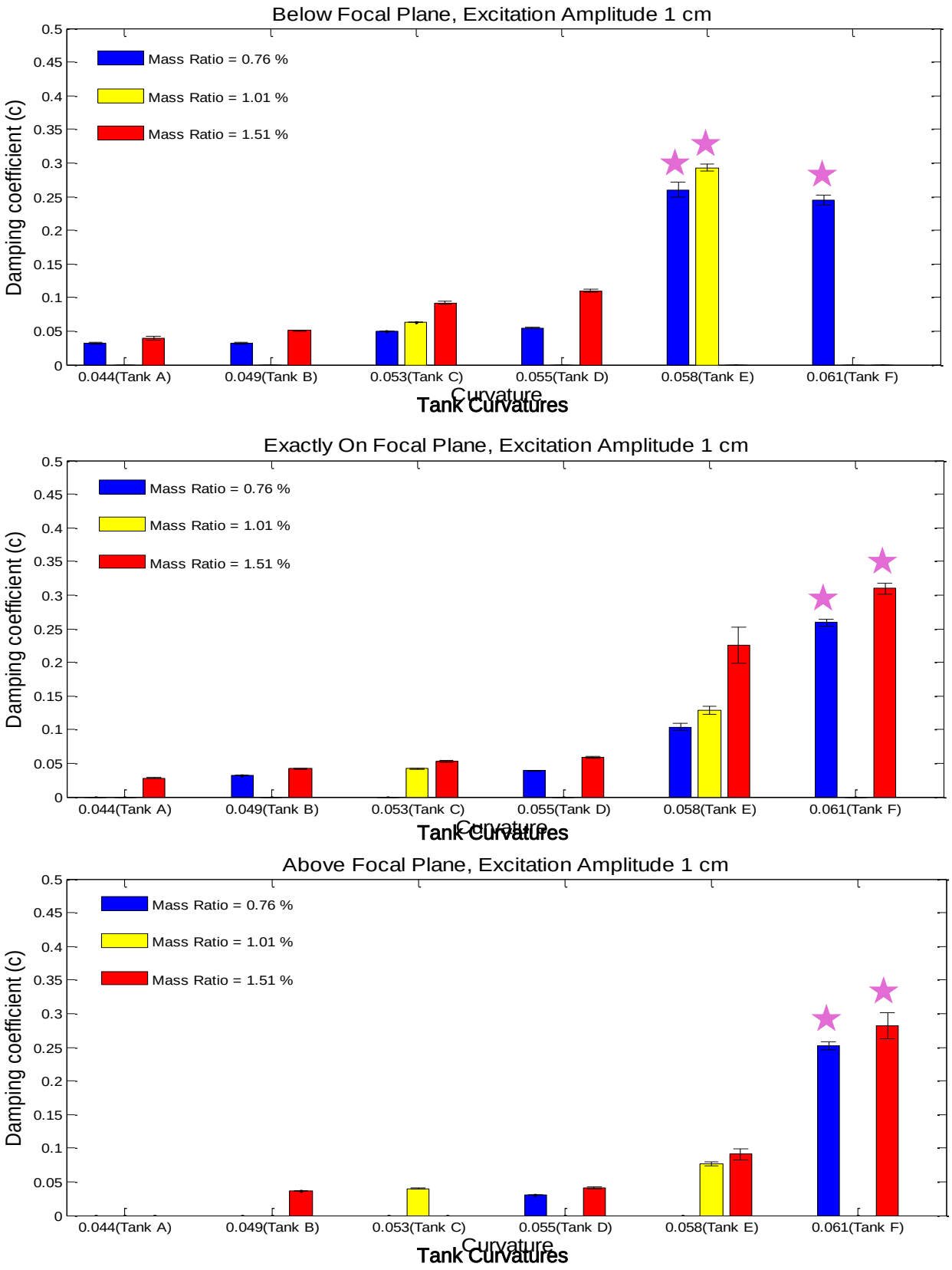

Fig. 5-4 Damping coefficient (c) of structure vibration with paraboloidal tank TLD (Tank A to F). All the setup initial excitation amplitudes of structure were 1 cm

★ denotes the occurrence of fluid rotation inside the TLD

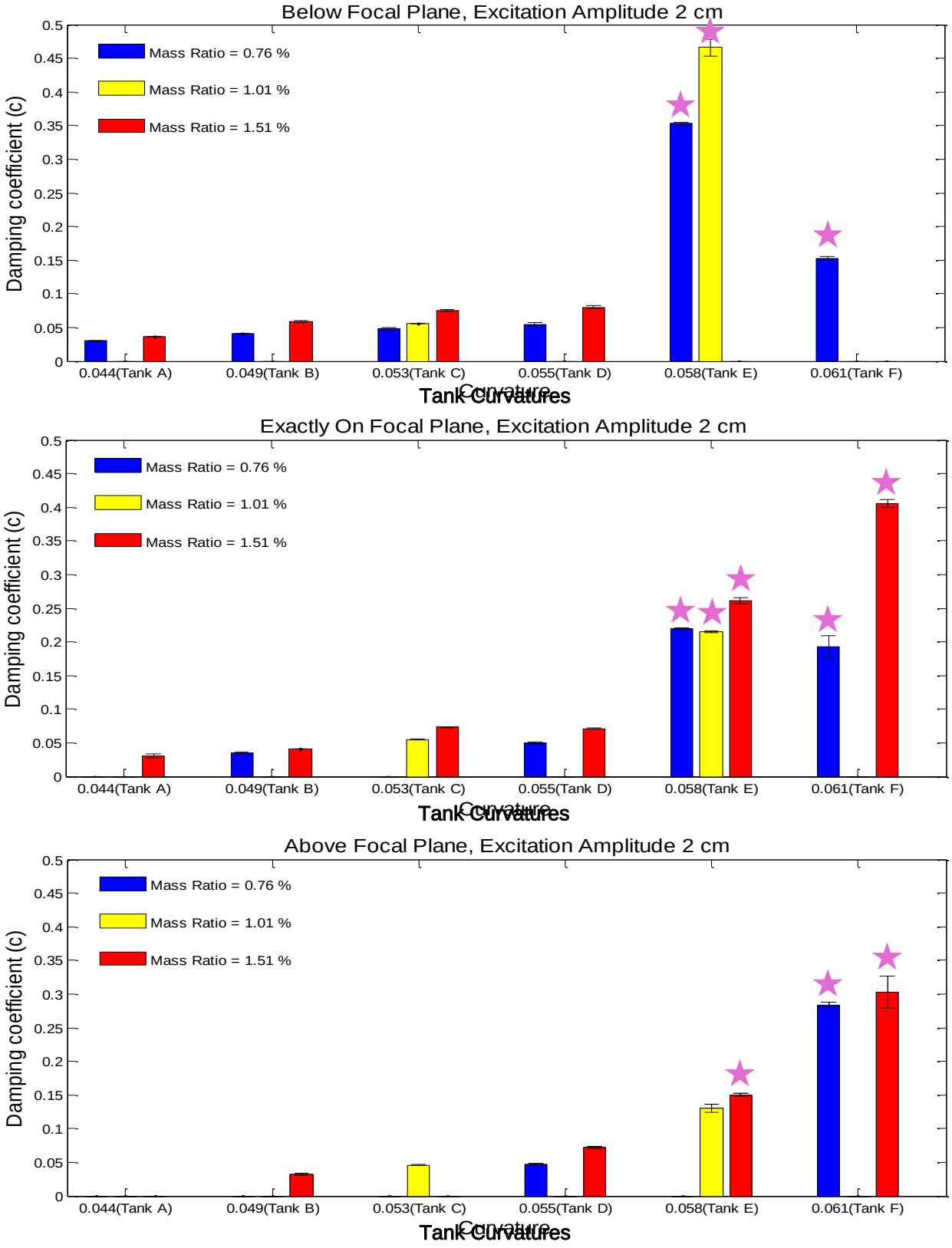

Fig. 5-5 Damping coefficient (c) of structure vibration with paraboloidal tank TLD (Tank A to F). All the setup excitation amplitudes of structure were 2 cm

★ denotes the occurrence of fluid rotation inside the TLD

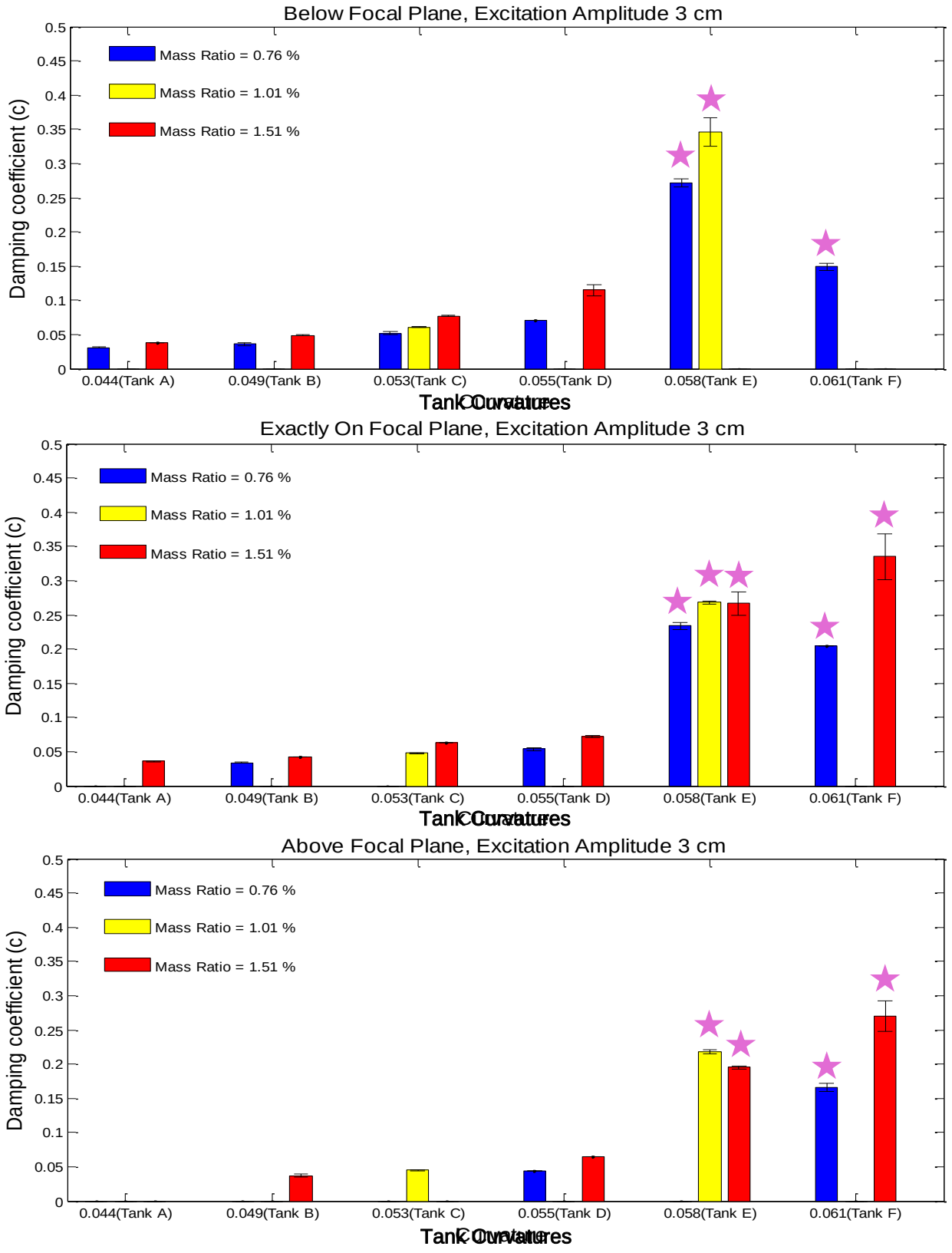

Fig. 5-6 Damping coefficient (c) of structure vibration with paraboloidal tank TLD (Tank A to F). All the setup excitation amplitudes of structure were 3 cm

★ denotes the occurrence of fluid rotation inside the TLD

Natural Frequencies of Fluid Sloshing and Rotation

In order to determine the optimal mitigation effects of structure vibration with paraboloidal tank TLD, it's necessary to measure the natural frequencies of water sloshing in different conditions.

After shaking the water tanks respectively for 3 times as excitation, we made all the water tanks at rest then started to measure the first-mode frequency of water sloshing named as f_w according to Equation (3.6). In addition, the frequencies of rotating fluid in Tank E and F were measured if exist. For the frequencies of structure vibration (f_s) one replaced the water by the same mass of weights, i.e., 90, 120, 180 grams corresponding to three water mass ratios of 0.76 %, 1.01 % and 1.51 %. Thus, the frequency ratio (FR) of water (f_w) to structure (f_s) is calculated as

$$\mathbf{FR} = \frac{f_w}{f_s} \tag{5.1}$$

Whenever the frequency ratio (FR) is close to 1, the resonance occurs approximately.

Fig. 5-7 (a) shows the frequency ratios of variation for six tank curvatures and three mass ratios before fluid rotation. The details of the experimental results are shown in Appendix 4. It indicates that if the curvatures of water tanks are larger (i.e. Tank E or F), the frequency ratios (FR) will get closer to 1 (of the values from 0.818 to 0.939 in Appendix 4), which is near the resonant condition. It will lead to the relatively intense fluid sloshing motion with breaking wave observed in the experiment. Accompanied with the turbulence flow, the fluid rotates around the tank boundary of TLD as seen in Fig. 5-8. During the fluid rotation in Tank E and F, the frequency ratios (FR) of rotating fluid to the structure are approximately equal to 1 (of the values from 0.939 to 1.054 in Fig. 5-7 (b) and the resonance occurred. With the rotation effects, the fluid in TLD will efficiently exert the anti-phase damping forces to mitigate the vibration in addition to fluid sloshing forces. It allows to explain why the fluid rotation in TLD can enhance the mitigation effects of structure vibration. Also, when the water surface level is set up below the focal plane, the frequency ratios of rotating fluid in Tank E (of the values from 0.981 to 0.983 in Fig. 5-7 (b) are closer to 1 than in Tank F (of the value of 1.054). Conversely, if the water surface level is set up exactly on or above the focal plane, the frequency ratios of rotating fluid in Tank F (of the values from 1.003 to 1.031) are closer to 1 than in Tank E (of the values from 0.939 to 0.963). It will lead to the better mitigation effects of structure vibration, which corresponds to the experimental results as illustrated in Fig. 5-4~5-6.

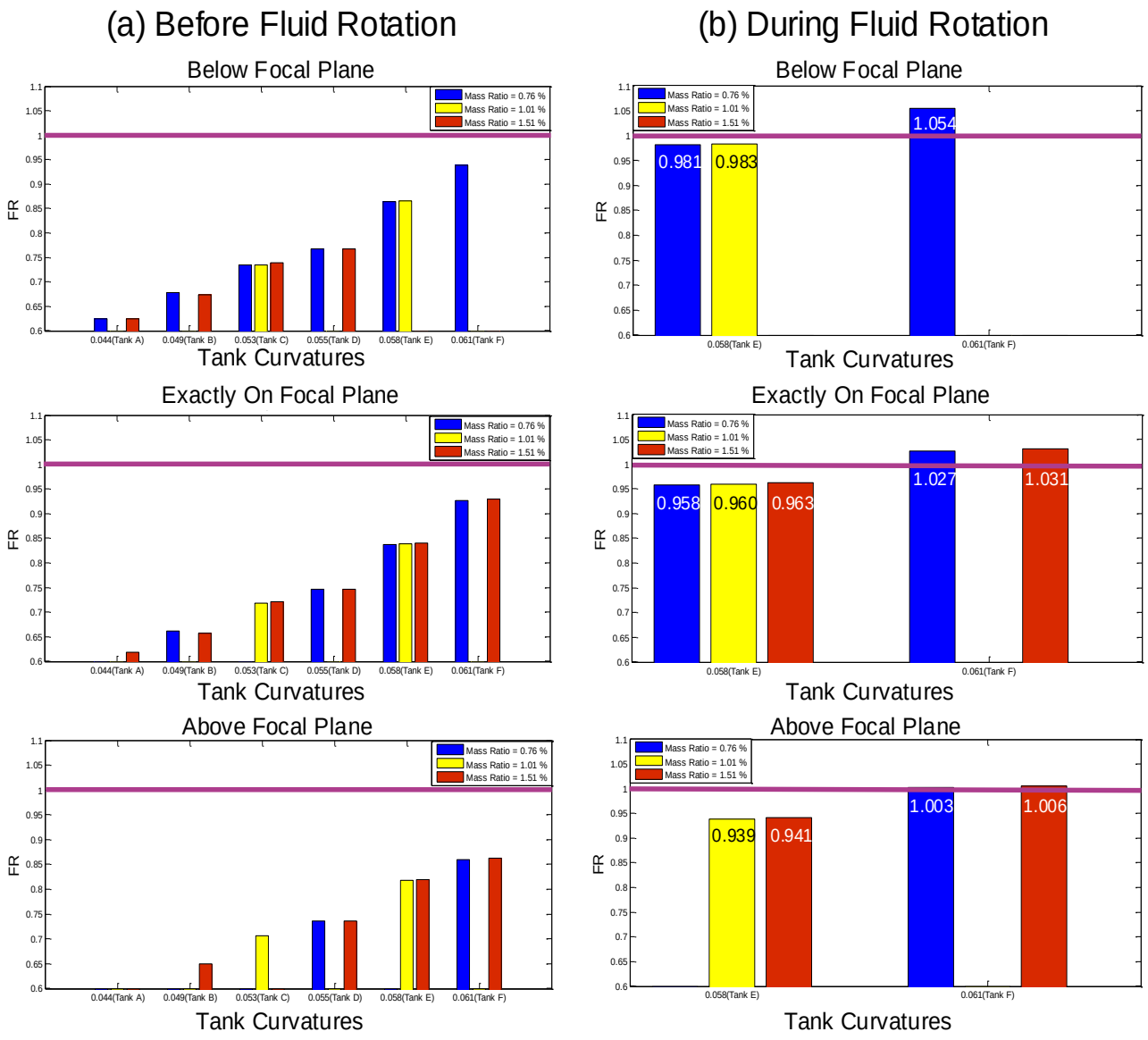

Fig. 5-7 (a) Frequency ratios (FR=f_w/f_s) of Tank A to F under three mass ratios before fluid rotation; (b) Frequency ratios (FR) of rotating fluid to structure (— Resonance, FR = 1)

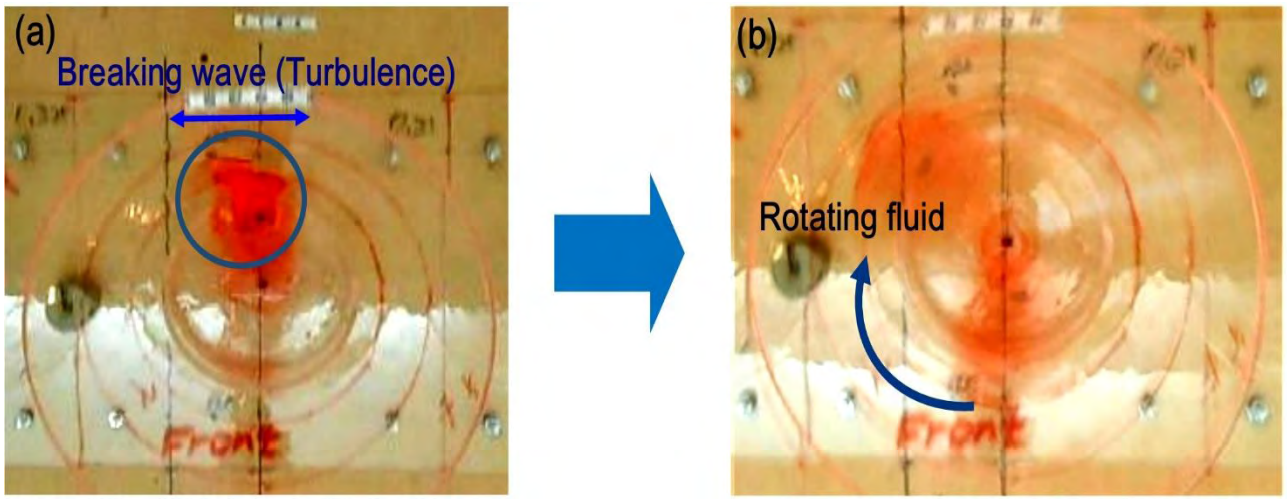

Fig. 5-8 Breaking wave within the blue circle in (a) accompanied with turbulence flow, which caused the fluid rotation in (b)

The Damping Forces Exerted by Rotating Fluid in TLD to the Structure (Tank E and F)

As discussed in last section, under the conditions of resonance in Tank E and F, the anti-phase damping forces can be efficiently generated by rotating fluid in TLD to mitigate the structure vibration. Doubtlessly, the magnitudes of the anti-phase damping forces may affect the mitigation of structure vibration. In this section, Tank E and F were assessed under different setup conditions of water surface levels and water mass ratios in which the fluid rotation occurred (as marked by ★ in Fig. 5-5, all the initial excitation amplitudes were set to 2 cm). Moreover, the displacements of the small particle moving along the tank wall enable to calculate the maximum acceleration (i.e., longitudinal component a_x, transverse component a_y and vertical component a_z in Fig. 5-9) of the fluid in "Tracker" before and during the rotation within first 10 seconds. This will be useful in analyzing the force magnitudes applied to this particle in the direction of structure vibration. The mitigation effects of structure vibration can also be evaluated by the damping coefficient (c) before and during the fluid rotation as illustrated in Fig. 5-10.

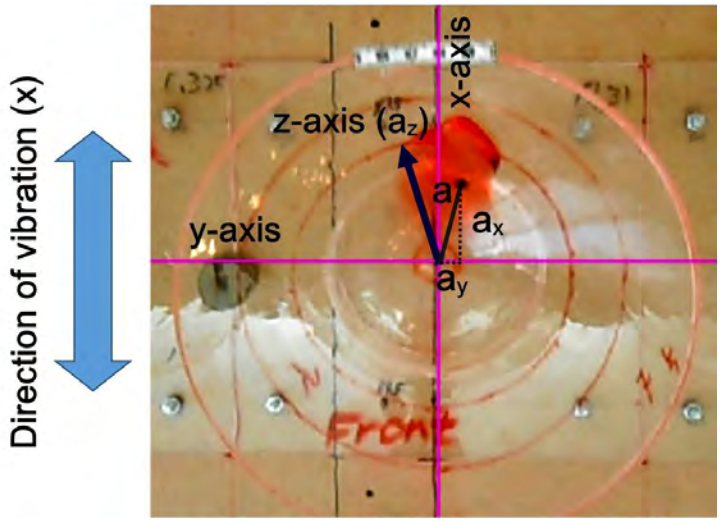

Fig. 5-9 The directions of the particle accelerations (a_x, a_y, a_z components)

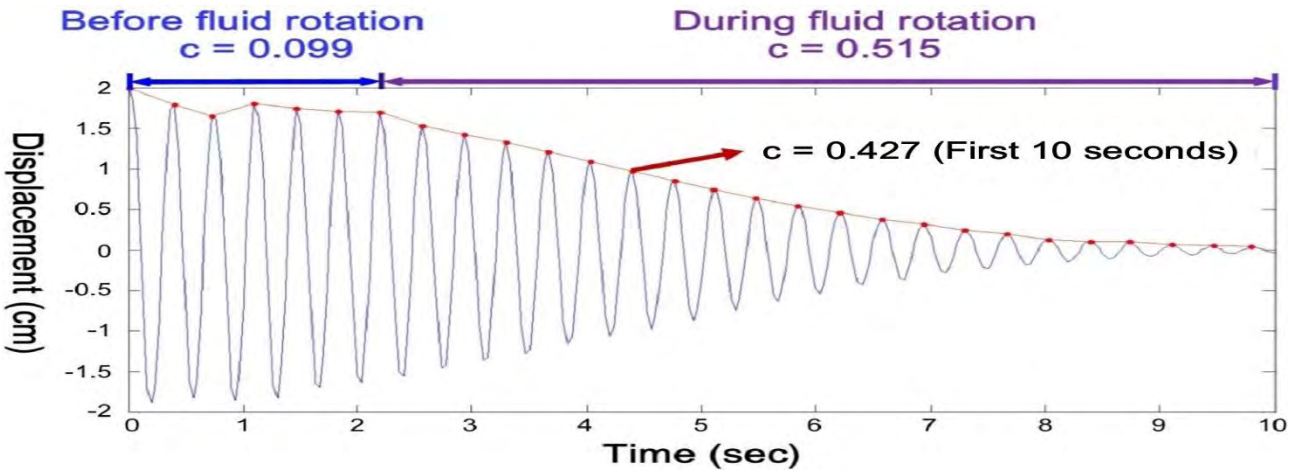

Fig. 5-10 The damping coefficient (c) of the structure vibration curve before (first 2 seconds) and during (first 2~10 seconds) the fluid rotation

Fig. 5-11, 5-12 show the maximum accelerations of the particle in Tank E, F and the damping coefficient (c) along the direction of structure vibration, before the fluid rotation (in Fig. 5-11 (a), 5-12 (a) and during the fluid rotation (in Fig. 5-11 (b), 5-12 (b). The details of the experimental results are shown in Appendix 5. Fig. 5-11 indicates that the maximum accelerations of the particle are larger as well during the fluid rotation than before the rotation. Further, Fig. 5-12 indicates that the damping coefficient (c) of structure vibration curve are 0.50~4.88 times larger in average as well during the fluid rotation than before the rotation. Those imply that the fluid rotation in TLD can indeed provide the larger damping forces to mitigate the structure vibration more efficiently. During the fluid rotation in TLD, the maximum accelerations of the particle in Tank E are larger than that in Tank F when the water surface level is set up below the focal plane (as seen in Fig. 5-11 (b). Conversely, if the water surface level is set up exactly on or above the focal plane, the maximum accelerations of the particle in Tank F will be larger than those in Tank E. It will lead to the larger damping forces to mitigate the structure vibration better, which corresponds to the experimental results as illustrated in Fig. 5-5.

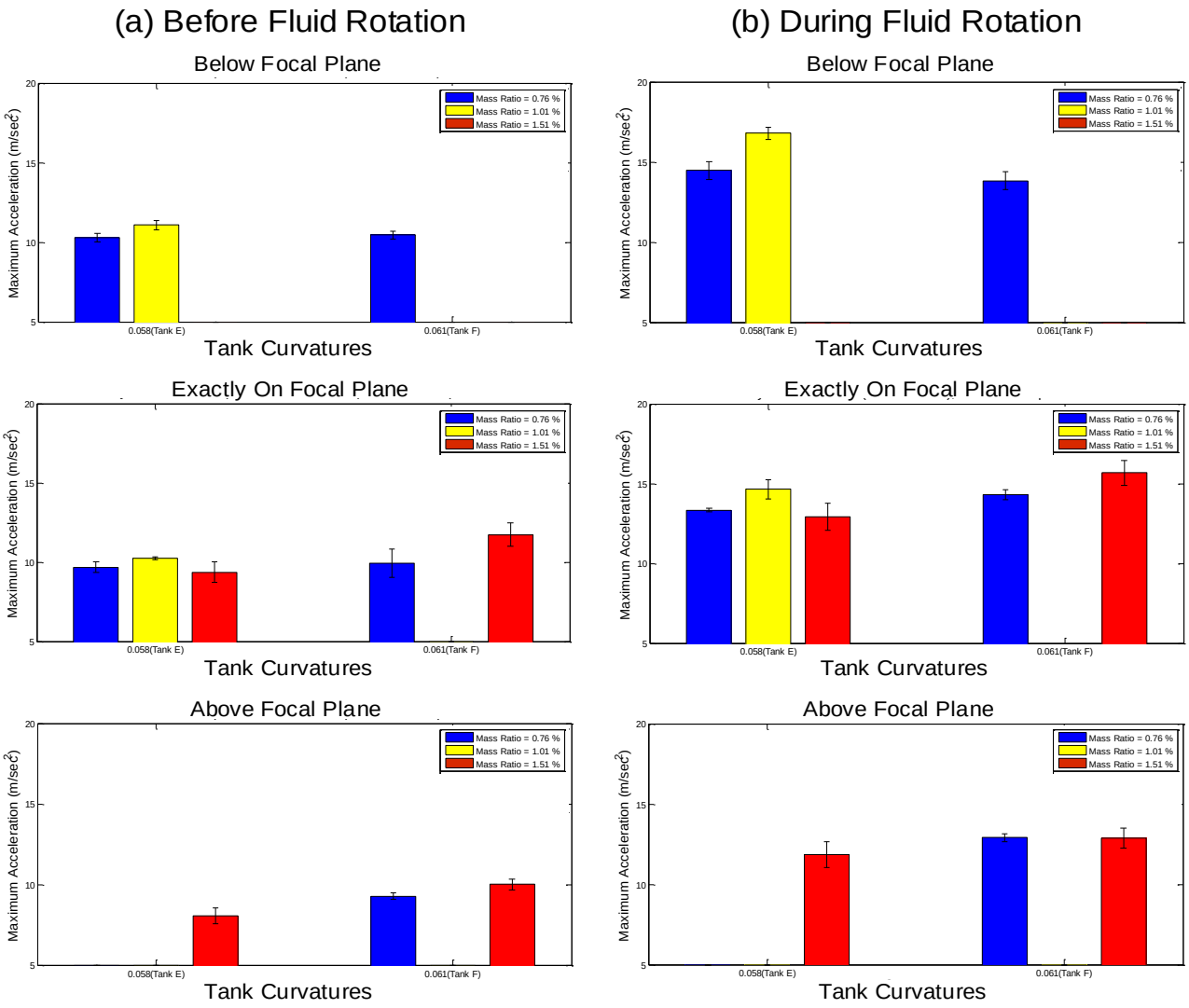

Fig. 5-11 The maximum accelerations of the particle before (a) and during (b) the fluid rotation (excitation amplitude 2 cm)

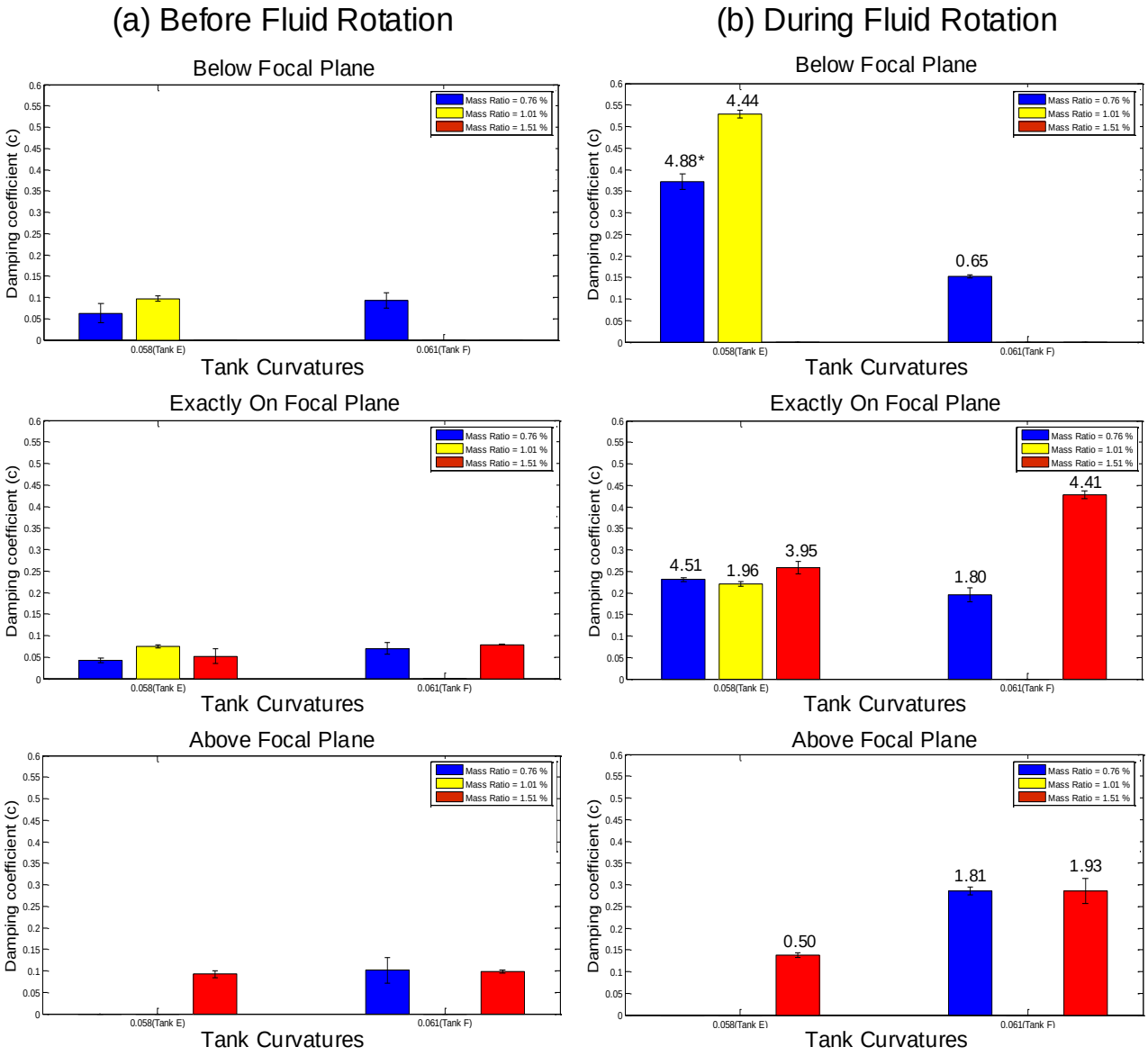

Fig. 5-12 The damping coefficient (c) of the structure vibration before (a) and during (b) the fluid rotation (excitation amplitude 2 cm)

* The increase rate of the damping coefficient (c) as well during fluid rotation (c_d) than before rotation (c_b) $= \frac{c_d - c_b}{c_b}$

To Evaluate the Magnitudes of Structure's Lateral Displacements Before and After the Installation of Flow-Guiding Vanes to Control the Direction of Fluid Rotation

The rotating fluid in TLD may provoke the lateral applied forces and accordingly the lateral displacements of structure, which is not predictable in orientation of rotation since the nonlinear instability of breaking wave is rather random. This will make adverse side effects for the use of TLD to mitigate the structure vibration. It becomes preferable to control the direction of fluid rotation so that the transverse vibration of structure is avoided. To this end, the submerged flow-guiding vanes (we will call it simply as guide vanes) of 1 cm high with 4 holes on the sides in order to reduce the extra interruption to the flow, as shown in Fig. 5-13, were installed on each tank bottom with 30 degrees of oblique angle. Fig. 5-14 shows the installation of guide vanes arranged either to the left or to the right of the main direction of vibration, which controls the fluid to rotate clockwise or counterclockwise effectively. In this experiment, the direction of fluid rotation in each water tank was controlled as alternately opposite to the adjacent ones, which may counteract the lateral applied forces in pairs to avoid the lateral displacements of structure. However, with the usage of unpaired water tanks (for example, three tanks were utilized; Tank E, the water surface levels were exactly on (mass ratio 0.76 %) and above (mass ratio 1.51 %) the focal plane), at least in one of the water tank the fluid will additionally rotate clockwise or counterclockwise even with guide vanes control. Which may not counteract the lateral applied forces between each other but also provoke the lateral displacements of structure.

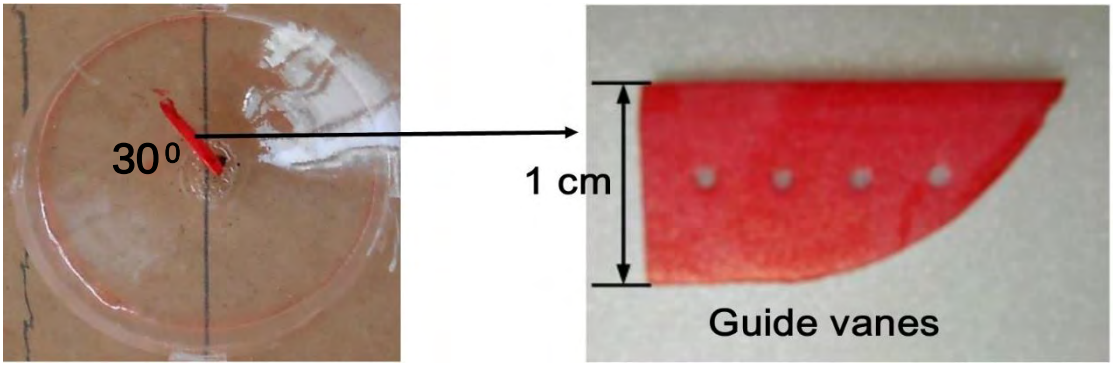

Fig. 5-13: Installation of guide vanes inside the water tanks

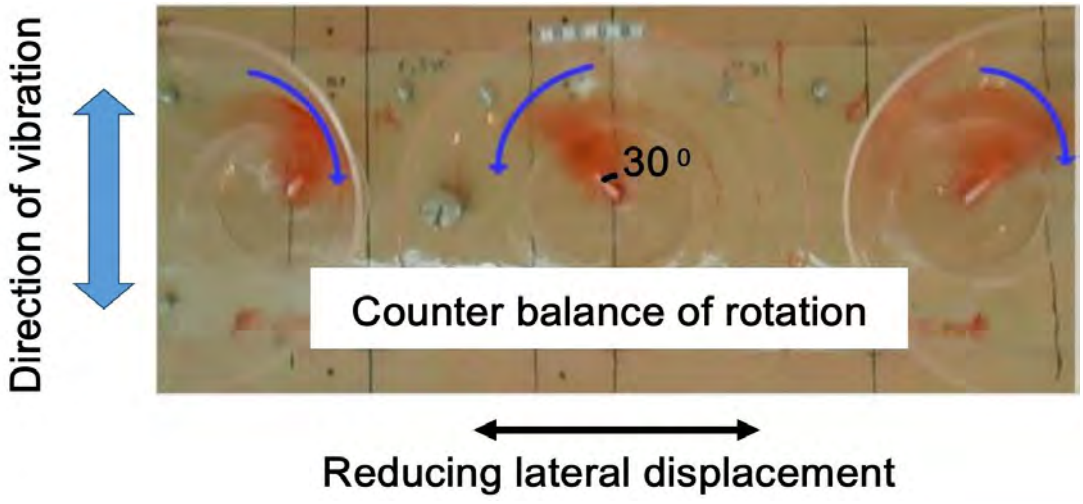

Fig. 5-14: The direction of fluid rotation in each tank

Each experiment was repeated five times for reproducibility. Both maximum structure lateral displacements before and after the installation of guide vanes in water tanks were measured and compared. Also, the direction of fluid rotation (clockwise or counterclockwise) in each tank was recorded with the "Rotation number (R)" to be acquired from Equation (5.2) for comparison.

$$R = \frac{|N^+ - N^-|}{N^+ + N^-} \tag{5.2}$$

where N^+= The amount of water tanks in which the fluid rotates clockwise; N^-= The amount of water tanks in which the fluid rotates counterclockwise; $N^+ + N^-$= Total amount of water tanks to be tested (see Table 4-1). If the Rotation number of TLD is equal or close to zero, it means the fluid in one half of water tanks rotates clockwise and in the others rotates counterclockwise. In this situation, the adverse lateral forces generated by fluid rotation in these tanks will counteract each other and the structure vibrates mainly in longitudinal direction with less transverse component effects. Otherwise, the net lateral force can be generated to exert on the structure transversely if R is close to 1. The side effects might sometimes threaten the safety of structure with TLD due to external loadings.

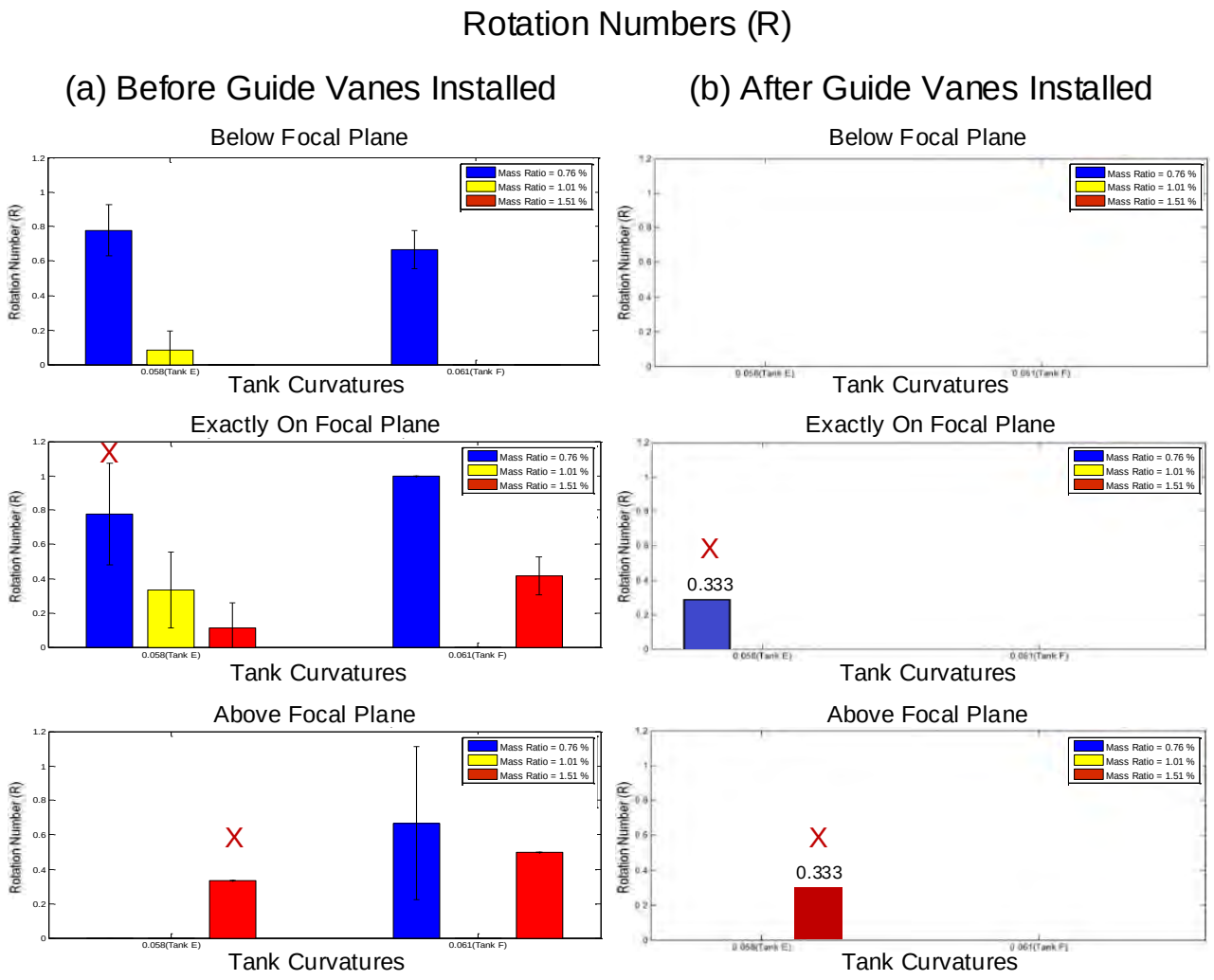

X: Unpaired water tanks (guide vanes)

Fig. 5-15: Rotation numbers by using Tank E and F for TLD before (a) and after (b) guide vanes installed (excitation amplitude 2 cm)

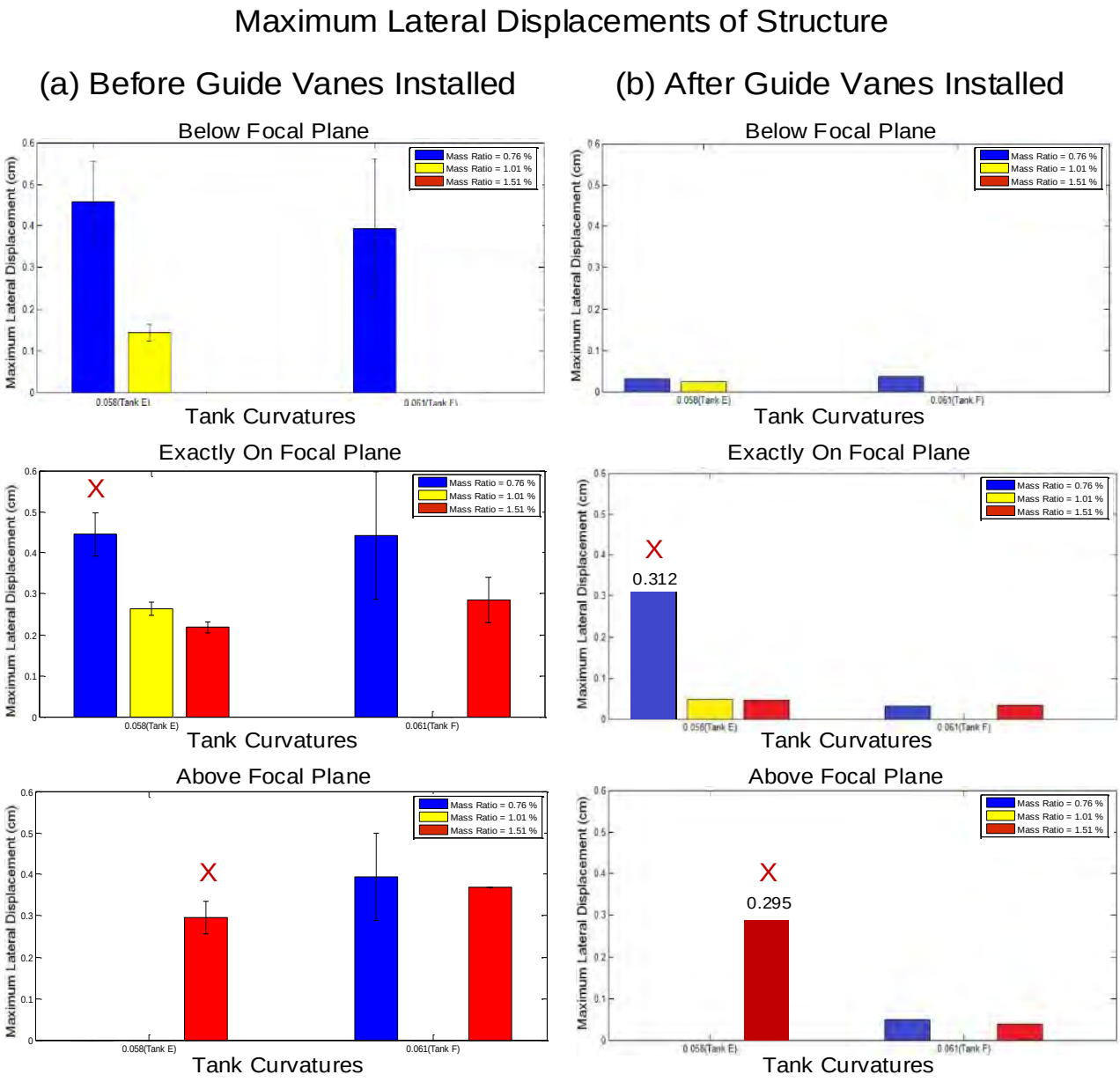

X: Unpaired water tanks (guide vanes)

Fig. 5-16: The maximum lateral displacements of structure before (a) and after (b) guide vanes installed (excitation amplitude 2 cm)

Fig. 5-15 shows the Rotation numbers by using Tank E and F for TLD and Fig. 5-16 shows the corresponding maximum lateral displacements of structure before (a) and after (b) the installation of guide vanes. Fig. 5-15 (a), 5-16 (a) illustrate the condition of unbalanced lateral forces exerted on the structure. The side effects were avoided for R close to zero and correspondingly the relatively smaller lateral displacements of structure were measured, as seen in Fig. 5-15 (b), 5-16 (b). However, some exceptional cases (marked with red X) were found as well in these figures for R to be far from zero, in which the unpaired water tanks (guide vanes) were applied for TLD. The lateral forces cannot be avoided in these cases even for the guide vanes being installed in the tanks. Therefore, the utility of paired water tanks with guide vanes for TLD is suggested. The details of the experimental results are shown in Appendix 6.

Chapter 6 Conclusions and Practical Applications

A series of experiments have been conducted in this study to investigate the mitigation effects of structure vibration with paraboloidal tank TLD. Using a simple homemade structure model equipped with multiple paraboloidal tanks as the TLD system. The mitigation effects of structure vibration were discussed through the variation of four setup parameters, including tank curvatures, water depths, water mass ratios and initial amplitudes of structure vibration. The research indicated that the optimal mitigation effects of structure vibration were achieved when the water depths inside the specific curvatures of paraboloidal tanks were all tuned up so that the natural frequencies of water sloshing is close to the frequency of structure vibration (near resonant condition). The relatively intense water sloshing motion combined with the occurrence of breaking wave were observed to induce the fluid rotation since the lateral forces exerted on the fluid. After the fluid rotation in TLD develops the periodical motion, its frequency in rotation is even closer and approximately equals to the frequency of structure vibration. The condition of resonance occurred so that the rotating fluid can exert the larger anti-phase longitudinal forces applied to mitigate the structure vibration at most 4.88 times better. Under these conditions, the larger the excitation amplitude of structure is, the more the possibility of fluid rotation occurred, and the better the mitigation effects of vibration will be achieved. Also, the larger mass ratio of liquid in TLD to structure leads to the better mitigation effects of vibration.

However, the fluid rotation in TLD will also randomly and adversely provoke the lateral applied forces and accordingly the lateral displacements of structure. To keep from this adversity, the submerged flow-guiding vanes with certain oblique angle were installed at the bottom of each water tank which can effectively control the desired orientation of fluid rotation. So that the fluid in a pair of TLD water tanks can counteract the lateral forces between each other to avoid the lateral displacements of structure.

The study illustrated that the paraboloidal tank TLD with paired auxiliary flow-guiding vanes is a useful damping device applied to mitigate the vibration of structure. This kind of TLD can be installed on the top of the building arranged as a circle of multiple pairs of water tanks. With the designs suggested in this study and the installation of guide vanes to control the direction of fluid rotation, the TLD can effectively mitigate the structure vibration under the horizontal excitation in arbitrary directions. It can also be combined with the designs of structure such as the water storage system or the liquid fuel tanks for liquid supply, fire emergency or many other purposes. Without extra loadings applied to the structure with TLD since it is usually a necessity for a structure system. It can also be applied as the nutation dampers of the dual-spin satellites, since the rotating fluid in TLD may counterbalance the nutation of satellites (shift its equilibrium spin axis) to stabilize its motion.

Chapter 7 References

[1] Tanuja P. B. and Radhey S. J. (2010), Duak-layer multiple tuned mass dampers for vibration control of structures, *International Journal of Advanced Structural Engineering*, Vol. 2, No. 2, Pages 91-113, December 2010.

[2] https://en.wikipedia.org/wiki/Tuned_mass_damper, Wikipedia.

[3] Emily B., Lipica H., Richi P. S. (2013), An experimental study on tuned liquid damper for mitigation of structural response, *International Journal of Advanced Structural Engineering* 2013, 5:3.

[4] Nishant K. R. (2013), *Water as energy absorber to control the seismic response of the structures*, PhD Thesis, Department of structural and seismic engineering, Mumbai University, India.

[5] https://en.wikipedia.org/wiki/Breaking_wave, Wikipedia.

[6] Banerji P., Murudi M., Shah A.H., Popplewell N. (2000), Tuned liquid dampers for controlling earthquake response of structures, *Earthquake Engineering and Structural Dynamics* 29:587–602.

[7] Hadi M. (2011), Experimental and analytical investigations of rectangular tuned liquid dampers (TLDs), Department of Civil Engineering, University of Toronto, Canada.

[8] Ibrahim R.A. (2005), Liquid sloshing dynamics theory and applications, Department of Mechanical Engineering, Wayne State University, USA, Cambridge University Press.

[9] Bauer H. F. (1984), Oscillations of immiscible liquids in a rectangular container, *Journal of Sound and Vibration*, Vol. 93(l), pp. 117-133.

[10] Sun L. M. (1991), Semi-analytical modeling of tuned liquid damper (TLD) with emphasis on damping of liquid sloshing, PhD Thesis, University of Tokyo, Japan.

[11] Sun L. M., Fujino Y., Pacheco M., Chaiseri P. (1992), Modelling of tuned liquid damper (TLD), *Journal of Wind Engineering and Industrial Aerodynamics*, pp. 41-44.

[12] Wakahara T., Ohyama T., Fujii K. (1992), Suppression of wind-induced vibration of a tall building using tuned liquid damper, *Journal of Wind Engineering and Industrial Aerodynamics*, 41-4.4, pp. 1895-1906.

[13] Tamura Y., Fujii K., Ohtsuki T., Wakahara T., Kohsaka R. (1995), Effectiveness of tuned liquid dampers under wind excitation, *Engineering Structures*, Vol. 17, No. 9, pp. 609-621.

[14] Ibrahim R. I., Li W. (1988), Parametric and autoparametric vibrations of an elevated water tower, part II: *Autoparametric response*, *Sound Vib*.121 (3), 429–444.

[15] Yu J.K. (1997), *Nonlinear characteristics of tuned liquid dampers*, PhD Thesis, Department of Civil Engineering, University of Washington, USA.

[16] Shigehiko K., Yasuo M. (2000), Dynamical modeling of deepwater-type cylindrical tuned liquid damper with a submerged net, *Journal of Pressure Vessel Technology*, 96 / Vol. 122, February 2000.

[17] Deng X., Tait M. J. (2009), Theoretical modeling of TLD with different tank geometries using linear long wave theory, *Journal of Vibration and Acoustics*, August 2009, Vol. 131/ 041014-1.

[18] Hassan M. (2010), *A numerical study of the performance of tuned liquid dampers*, Master

Thesis, Department of Applied Science (Mechanical Engineering), McMaster University, Hamilton, Ontario, Canada.
[19] https://en.wikipedia.org/wiki/Wave_shoaling, Wikipedia.
[20] Bauer H. F. (1984d), Forced liquid oscillations in paraboloid-containers, *Zeit, fur Flugwissenschaften und Weltraumforschung***8**, 49–55.
[21] Bauer H. F. (1999), Oscillations of non-viscous liquid in various container geometries, *Forschungbericht* LRT-WE-9-FB-1.
[22] https://en.wikipedia.org/wiki/Mean_curvature, Wikipedia.

Appendix

1 The Designs of Paraboloidal Tanks and the Verification of Accuracy

(1) To Determine the Size of Paraboloidal Tanks under Six Different Curvatures

First, we supposed that six different curvatures of paraboloidal tanks filled with 180, 90, 60, 45, 30, 22.5 ml of water respectively in which the water surface levels will reach the focal plane. The volume (V) of water in the paraboloidal tank

$$z = f(x,y) = \frac{x^2+y^2}{4p} \quad \text{(a.1)}$$

where z is the height and p is the vertical distance from vertex to focal plane of paraboloidal tank, can be expressed as

$$V = \int_0^p A(z)\,dz = \int_0^p \pi(x^2+y^2)\,dz = \int_0^p 4p\pi z\,dz = 2p\pi z^2\,|_0^p = 2\pi p^3 \quad \text{(a.2)}$$

We got six different values of p by substituting six different volumes of water (V = 180, 90, 60, 45, 30, 22.5 ml) into Equation (a.2) respectively. The design parameters of paraboloidal tanks under six different curvatures were acquired (3.17).

(2) To Verify the Accuracy of Paraboloidal Tanks

First, we chose one section (in the direction of structure vibration/ Fig. a-1) in each of the paraboloidal tank. Then, filled with certain depths of water for every 1 cm (1, 2, 3 …..12 cm) and started to measure the radius of water surface (X_m) within the section (Fig. a-1). Compared to the theoretical value (X) according to the original designs of water tanks (see Table 4-1), the Coefficient of determination (r^2) can be expressed as

$$r^2 = 1 - \frac{\sum(X_m - X)^2}{\sum(X - \bar{X})^2} \quad \text{(a.3)}$$

where X_m is the measured radius of water surface within the section, X is the theoretical value of the radius of water surface and $\bar{X}$ is the average of the theoretical values.

If the Coefficient of determination (r^2) is over **0.97**, the accuracy of the paraboloidal tank is acceptable.

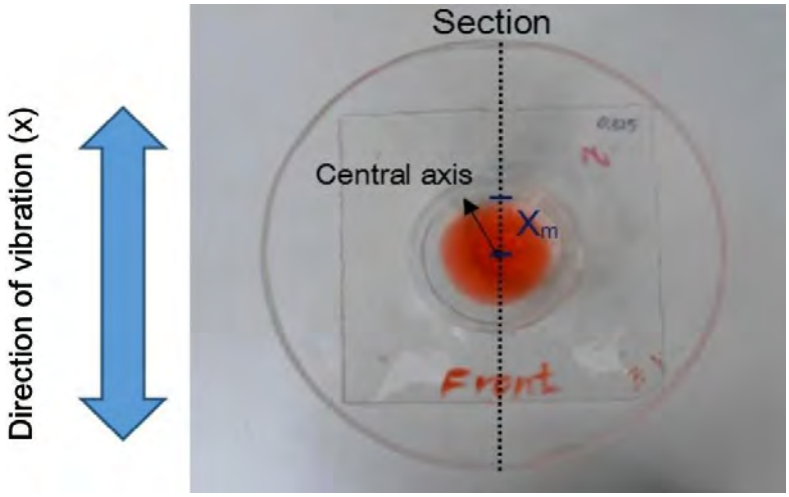

Fig. a-1: The section of the paraboloidal tank and the measurement of X_m

After the verification, we found that the accuracies of all the paraboloidal tanks as used in this experiment are acceptable (r^2>0.97).

Table a-1 The Coefficient of Determination (r^2) of all the Paraboloidal Tanks							
Tank Curvatures	**Amount of Water Tanks**	**Serial Numbers**	**r^2**	**Tank Curvatures**	**Amount of Water Tanks**	**Serial Numbers**	**r^2**
0.044 (Tank A)	**2**	**A1**	**0.992**	**0.058 (Tank E)**	**8**	**E1**	**0.996**
		A2	**0.993**			**E2**	**0.998**
0.049 (Tank B)	**4**	**B1**	**0.998**			**E3**	**0.998**
		B2	**0.998**			**E4**	**0.998**
		B3	**0.996**			**E5**	**0.999**
		B4	**0.999**			**E6**	**1.000**
0.053 (Tank C)	**6**	**C1**	**0.992**			**E7**	**0.999**
		C2	**0.996**			**E8**	**0.999**
		C3	**0.997**	**0.061 (Tank F)**	**8**	**F1**	**0.988**
		C4	**0.999**			**F2**	**0.978**
		C5	**0.999**			**F3**	**0.994**
		C6	**0.999**			**F4**	**0.989**
0.055 (Tank D)	**8**	**D1**	**1.000**			**F5**	**0.997**
		D2	**1.000**			**F6**	**0.996**
		D3	**0.999**			**F7**	**0.993**
		D4	**0.998**			**F8**	**0.987**
		D5	**0.999**				
		D6	**1.000**				
		D7	**1.000**				
		D8	**0.999**				

2 Matlab codes

(1) Continuous Wavelet Transform of Structure Vibration Curve

```
clear all;
S = xlsread('Analysis','Sheet1'); % import the experimental results from the file 'Analysis' in Sheet 1
%----------------------------------

for i = 1:5; % five times of experiments
x = S(:,2*i); % displacement data of structure vibration
L = length(x); % sampling amount
Fs = 30; % sampling frequency
T = 1/Fs;
to = (0:L-1)*T;
t = flipud(rot90(to)); % time axis of wavelet plot
wname = 'morl'; % the type of mother wavelet function (Morlet)
scales = 1:0.125:256; % the scale of wavelet function
coefs = cwt(x, scales, wname); % execute continuous wavelet transform then acquire wavelet modulus
freq = scal2frq(scales, wname ,1/Fs); % frequency axis of wavelet plot
figure(i);
surf (t, freq, coefs); % 3D wavelet plot (wavelet modulus against time, frequency)
%----------------------------------

mod_coefs = flipud(rot90(coefs));
[peak_mod, ind] = max(sum(mod_coefs.^2));
acq = mod_coefs(:, ind);
[pks, locs] = findpeaks(acq);
TT = (locs-1)*T; % extract the singlet peak from wavelet plot under the certain frequency condition
[pks2, locs2] = findpeaks(pks);
pks(1:locs2-1, :) = [];
TT (1:locs2-1, :) = [];
f=fit(TT, pks,'exp1') % curve fitting of singlet peak (exponential fit)
figure(i+5);
plot(f, TT, pks) % plot the figure of singlet peak against time with regression line
end
```

(2) To Solve the Equation in Matlab

From Equation (4.7): $2\sqrt{p}\frac{D}{H}\cdot z^{1.5} + 2\sqrt{p}\cdot z^{0.5} - r_m = 0$

Provide a =$2\sqrt{p}$, b =$\frac{D}{H}$, c = r_m, x = $\sqrt{z}$

```
syms a b c x
eqn = a*b*x^3 + a*x-c == 0;
solx = solve(eqn, x)                % solve the value of x
vpa(solx.^2)                        % show the value of x^2 (z)
```

```
ans =
(((0.0370/b^3 + (0.25*c^2)/(a^2*b^2))^(1/2) + (0.5*c)/(a*b))^(1/3) - 0.3333/(b*((0.0370/b^3 + …
(0.25*c^2)/(a^2*b^2))^(1/2) + (0.5*c)/(a*b))^(1/3)))^2     % the value of x^2 (z)
```

(3) To Make the Animation in Matlab

```
clc,clf, format compact
fid=fopen('location.txt','r');
formatspec='%f %f %f';
sizeA=[3 inf];
A=fscanf(fid,formatspec,sizeA);
x=A(1,:);y=A(2,:);z=A(3,:);
sizx=size(x,2)        % reading particle positions data under x, y, z dimensions from the file 'location.txt'
%---------------------------------

for j = 1:sizx
plot3(x(j),y(j),z(j),'o','MarkerFaceColor','r','MarkerSize',10);axis off; %3D plot of particle positions
axis([-5 5 -5 5 0 5]); xlabel('x');ylabel('y');zlabel('z');hold on            % add axis
quiver3(0,-5,1,3,0,0, 'LineWidth',3,'Color',[1 0 0], 'MaxHeadSize', 0.5) ;
quiver3(0,-5,1,-3,0,0, 'LineWidth',3,'Color',[1 0 0], 'MaxHeadSize', 0.5);
text(-4,-6,1,'Direction of Structure Vibration', 'Rotation', 14)            % to show the words ‘Direction of
 Structure vibration’ under 14 degrees of oblique angle and with a red double arrow above
%---------------------------------

for r = linspace (-7,7, 110)
theta= linspace(0, 2*pi, 60)
[r, theta] = meshgrid(r, theta)
a = r.*cos(theta)
b = r.*sin(theta)
c = r.^2/12.241
plot3(a, b, c, 'c');axis off; hold on
alpha(0.03); hold on
end                                % the for loop of plotting the paraboloidal tank background (i.e. Tank A)
%---------------------------------

s=sprintf('t = %4.3f',(j-1)/30);     % to show the corresponding time of particle positions
text (1,5,4,s); hold off
F(j) = getframe;                     % to get each of the frames in the animation
end

movie(F,2, 15)                       % to play the animation 15 frames per second for two times
movie2avi(F, 'playmovieA')           % to save the animation as “avi” file, named ‘playmovieA’
```

3 Damping Coefficient (c) of Structure Vibration (Detailed Tables)

Table a-2 Damping Coefficient (c) of Structure Vibration (Excitation Amplitude 1 cm)

	Tank Curvatures / Mass Ratios	0.044 (Tank A)	0.049 (Tank B)	0.053 (Tank C)	0.055 (Tank D)	0.058 (Tank E)	0.061 (Tank F)
Below Focal Plane	0.76 %	**0.032**/0.001	**0.032**/0.001	**0.050**/0.000	**0.055**/0.001	**0.260**/0.011	**0.245**/0.007
	1.01 %			**0.063**/0.000		**0.293**/0.005	
	1.51 %	**0.040**/0.003	**0.051**/0.001	**0.092**/0.002	**0.110**/0.002		
Exactly On Focal Plane	0.76 %		**0.032**/0.000		**0.039**/0.001	**0.104**/0.005	**0.259**/0.005
	1.01 %			**0.042**/0.001		**0.129**/0.006	
	1.51 %	**0.042**/0.001	**0.042**/0.001	**0.053**/0.001	**0.059**/0.001	**0.225**/0.027	**0.310**/0.008
Above Focal Plane	0.76 %				**0.031**/0.000		**0.252**/0.006
	1.01 %			**0.040**/0.001		**0.076**/0.003	
	1.51 %		**0.036**/0.000		**0.041**/0.001	**0.091**/0.008	**0.282**/0.019

Table a-3 Damping Coefficient (c) of Structure Vibration (Excitation Amplitude 2 cm)

	Tank Curvatures / Mass Ratios	0.044 (Tank A)	0.049 (Tank B)	0.053 (Tank C)	0.055 (Tank D)	0.058 (Tank E)	0.061 (Tank F)
Below Focal Plane	0.76 %	**0.030**/0.001	**0.041**/0.000	**0.048**/0.002	**0.055**/0.002	**0.353**/0.002	**0.152**/0.003
	1.01 %			**0.056**/0.000		**0.466**/0.013	
	1.51 %	**0.037**/0.000	**0.059**/0.001	**0.075**/0.001	**0.080**/0.002		
Exactly On Focal Plane	0.76 %		**0.035**/0.001		**0.050**/0.001	**0.219**/0.002	**0.193**/0.016
	1.01 %			**0.055**/0.001		**0.215**/0.001	
	1.51 %	**0.030**/0.003	**0.041**/0.000	**0.073**/0.001	**0.071**/0.001	**0.261**/0.005	**0.405**/0.006
Above Focal Plane	0.76 %				**0.047**/0.001		**0.284**/0.004
	1.01 %			**0.046**/0.001		**0.130**/0.006	
	1.51 %		**0.032**/0.002		**0.072**/0.001	**0.150**/0.002	**0.303**/0.024

Table a-4 Damping Coefficient (c) of Structure Vibration (Excitation Amplitude 3 cm)

	Tank Curvatures / Mass Ratios	0.044 (Tank A)	0.049 (Tank B)	0.053 (Tank C)	0.055 (Tank D)	0.058 (Tank E)	0.061 (Tank F)
Below Focal Plane	0.76 %	**0.031/0.001**	**0.036/0.002**	**0.052/0.002**	**0.071/0.000**	**0.272/0.006**	**0.149/0.005**
	1.01 %			**0.061/0.001**		**0.346/0.021**	
	1.51 %	**0.038/0.000**	**0.049/0.001**	**0.077/0.001**	**0.115/0.008**		
Exactly On Focal Plane	0.76 %		**0.034/0.001**		**0.054/0.002**	**0.234/0.005**	**0.204/0.000**
	1.01 %			**0.048/0.001**		**0.268/0.002**	
	1.51 %	**0.036/0.001**	**0.042/0.000**	**0.063/0.000**	**0.072/0.002**	**0.267/0.017**	**0.335/0.033**
Above Focal Plane	0.76 %				**0.044/0.000**		**0.116/0.006**
	1.01 %			**0.045/0.001**		**0.218/0.003**	
	1.51 %		**0.037/0.002**		**0.064/0.000**	**0.195/0.002**	**0.270/0.022**

* a/b: a. Damping coefficient (c); b. Standard deviation

4 Frequency Ratios (FR) of Water to Structure (Detailed Tables)

Table a-5 Frequency Ratios (FR) of Water to Structure/ Before Fluid Rotation							
	Tank Curvatures / Mass Ratios	0.044 (Tank A)	0.049 (Tank B)	0.053 (Tank C)	0.055 (Tank D)	0.058 (Tank E)	0.061 (Tank F)
Below Focal Plane	0.76 %	0.625	0.678	0.735	0.767	0.864	0.939
	1.01 %			0.735		0.866	
	1.51 %	0.625	0.674	0.739	0.767		
Exactly On Focal Plane	0.76 %		0.662		0.746	0.838	0.927
	1.01 %			0.719		0.839	
	1.51 %	0.618	0.658	0.722	0.746	0.841	0.930
Above Focal Plane	0.76 %				0.736		0.860
	1.01 %			0.707		0.818	
	1.51 %		0.650		0.736	0.820	0.863

Table a-6 Frequency Ratios (FR) of Water to Structure/ During Fluid Rotation			
	Tank Curvatures / Mass Ratios	0.058 (Tank E)	0.061 (Tank F)
Below Focal Plane	0.76 %	0.981	1.054
	1.01 %	0.983	
	1.51 %		
Exactly On Focal Plane	0.76 %	0.958	1.027
	1.01 %	0.960	
	1.51 %	0.963	1.031
Above Focal Plane	0.76 %		1.003
	1.01 %	0.939	
	1.51 %	0.941	1.006

5 The Maximum Accelerations of the Particle Before and During the Fluid Rotation under the Direction of Structure Vibration (Excitation Amplitude 2 cm) (Detailed Tables)

Table a-7 The Maximum Accelerations of the Particle (m/s^2)/ Before Fluid Rotation			
	Tank Curvatures / Mass Ratios	0.058 (Tank E)	0.061 (Tank F)
Below Focal Plane	0.76 %	**10.296**/0.260	**10.458**/0.244
	1.01 %	**11.080**/0.287	
	1.51 %		
Exactly On Focal Plane	0.76 %	**9.685**/0.348	**9.937**/0.898
	1.01 %	**10.255**/0.081	
	1.51 %	**9.374**/0.668	**11.734**/0.747
Above Focal Plane	0.76 %		**9.277**/0.192
	1.01 %		
	1.51 %	**8.059**/0.493	**10.010**/0.339

Table a-8 The Maximum Accelerations of the Particle (m/s^2)/ During Fluid Rotation			
	Tank Curvatures / Mass Ratios	0.058 (Tank E)	0.061 (Tank F)
Below Focal Plane	0.76 %	**14.475**/0.562	**13.839**/0.552
	1.01 %	**16.786**/0.392	
	1.51 %		
Exactly On Focal Plane	0.76 %	**13.347**/0.132	**14.311**/0.294
	1.01 %	**14.650**/0.591	
	1.51 %	**12.928**/0.852	**15.671**/0.766
Above Focal Plane	0.76 %		**12.918**/0.244
	1.01 %		
	1.51 %	**11.854**/0.788	**12.873**/0.626

* a/b: a. Maximum acceleration of the particle; b. Standard deviation

The Damping Coefficient (c) of the Structure Vibration Before and During the Fluid Rotation

Table a-9 The Damping Coefficient (c) of Structure Vibration/ Before Fluid Rotation			
	Tank Curvatures / Mass Ratios	0.058 (Tank E)	0.061 (Tank F)
Below Focal Plane	0.76 %	**0.063**/0.022	**0.092**/0.018
	1.01 %	**0.097**/0.006	
	1.51 %		
Exactly On Focal Plane	0.76 %	**0.042**/0.005	**0.070**/0.014
	1.01 %	**0.075**/0.004	
	1.51 %	**0.052**/0.017	**0.079**/0.001
Above Focal Plane	0.76 %		**0.101**/0.029
	1.01 %		
	1.51 %	**0.092**/0.008	**0.098**/0.004

Table a-10 The Damping Coefficient (c) of Structure Vibration/ During Fluid Rotation			
	Tank Curvatures / Mass Ratios	0.058 (Tank E)	0.061 (Tank F)
Below Focal Plane	0.76 %	**0.372**/0.018	**0.152**/0.003
	1.01 %	**0.529**/0.009	
	1.51 %		
Exactly On Focal Plane	0.76 %	**0.231**/0.005	**0.196**/0.016
	1.01 %	**0.221**/0.005	
	1.51 %	**0.259**/0.014	**0.428**/0.009
Above Focal Plane	0.76 %		**0.285**/0.009
	1.01 %		
	1.51 %	**0.138**/0.005	**0.286**/0.029

* a/b: a. Damping coefficient (c); b. Standard deviation

Table a-11 The Increase Rates of Damping Coefficient (c)			
	Tank Curvatures / Mass Ratios	0.058 (Tank E)	0.061 (Tank F)
Below Focal Plane	0.76 %	**4.88**	**0.65**
	1.01 %	**4.44**	
	1.51 %		
Exactly On Focal Plane	0.76 %	**4.51**	**1.80**
	1.01 %	**1.96**	
	1.51 %	**3.95**	**4.41**
Above Focal Plane	0.76 %		**1.81**
	1.01 %		
	1.51 %	**0.50**	**1.93**

* The increase rate of damping coefficient (c) during fluid rotation (c_d) than before rotation (c_b) = $\frac{c_d - c_b}{c_b}$

6 The Rotation Numbers (R) of TLD (Table a-12, a-13) and the Corresponding Maximum Lateral Displacements of Structure (Table a-14, a-15) (Excitation Amplitude 2 cm)

Table a-12 The Rotation Numbers (R) of TLD/ Before Guide Vanes Installed			
	Tank Curvatures / Mass Ratios	0.058 (Tank E)	0.061 (Tank F)
Below Focal Plane	0.76 %	**0.778**/0.148	**0.667**/0.111
	1.01 %	**0.083**/0.111	
	1.51 %		
Exactly On Focal Plane	0.76 %	**0.778**/0.296 X	**1.000**/0.000
	1.01 %	**0.333**/0.222	
	1.51 %	**0.111**/0.148	**0.417**/0.111
Above Focal Plane	0.76 %		**0.667**/0.444
	1.01 %		
	1.51 %	**0.333**/0.000 X	**0.500**/0.000

Table a-13 The Rotation Numbers (R) of TLD/ After Guide Vanes Installed			
	Tank Curvatures / Mass Ratios	0.058 (Tank E)	0.061 (Tank F)
Below Focal Plane	0.76 %	**0.000**/0.000	**0.000**/0.000
	1.01 %	**0.000**/0.000	
	1.51 %		
Exactly On Focal Plane	0.76 %	**0.333**/0.000 X	**0.000**/0.000
	1.01 %	**0.000**/0.000	
	1.51 %	**0.000**/0.000	**0.000**/0.000
Above Focal Plane	0.76 %		**0.000**/0.000
	1.01 %		
	1.51 %	**0.333**/0.000 X	**0.000**/0.000

* a/b: a. Rotation number (R); b. Standard deviation; X: Unpaired water tanks (guide vanes)

Table a-14 Maximum Lateral Displacements of Structure (cm)/ Before Guide Vanes Installed			
	Tank Curvatures / Mass Ratios	**0.058 (Tank E)**	**0.061 (Tank F)**
Below Focal Plane	**0.76 %**	**0.458**/0.097	**0.394**/0.166
	1.01 %	**0.144**/0.020	
	1.51 %		
Exactly On Focal Plane	**0.76 %**	**0.445**/0.053 **X**	**0.442**/0.156
	1.01 %	**0.264**/0.016	
	1.51 %	**0.218**/0.014	**0.285**/0.055
Above Focal Plane	**0.76 %**		**0.394**/0.106
	1.01 %		
	1.51 %	**0.295**/0.039 **X**	**0.368**/0.056

Table a-15 Maximum Lateral Displacements of Structure (cm)/ After Guide Vanes Installed			
	Tank Curvatures / Mass Ratios	**0.058 (Tank E)**	**0.061 (Tank F)**
Below Focal Plane	**0.76 %**	**0.031**/0.000	**0.037**/0.000
	1.01 %	**0.024**/0.000	
	1.51 %		
Exactly On Focal Plane	**0.76 %**	**0.312**/0.000 **X**	**0.032**/0.000
	1.01 %	**0.048**/0.000	
	1.51 %	**0.045**/0.000	**0.033**/0.000
Above Focal Plane	**0.76 %**		**0.050**/0.000
	1.01 %		
	1.51 %	**0.295**/0.000 **X**	**0.038**/0.000

* a/b: a. Maximum lateral displacement; b. Standard deviation; X: Unpaired water tanks (guide vanes)

【評語】100007

1. 本作品能從一篇理論論文出發、思考 Paraboloidal Tank Tuned Liquid Damper (TLD)對結構阻尼的效率，在整體應用的考量上，相當有潛在的應用價值。

2. 阻尼器一般而言有相當強的頻率效應，若能針對此部份作進一步的探討將可使本作品更具價值。除此之外，TLD 與更傳統的 mass-spring-dashpot 系統的比較也應有所比較。